Finite Element Based Design and Analysis of Unpaved Roads over Difficult Subsoil: Sustainable Application of Geotextile Reinforcement to Attain Long-Term Performance

Nayan Jyoti Sarma, Arindam Dey

Nayan Jyoti Sarma
Research Scholar, Department of Civil Engineering, Indian Institute of Technology Guwahati, India.
Email: nayan.jyoti@iitg.ac.in

Arindam Dey*
Associate Professor, Department of Civil Engineering, Indian Institute of Technology Guwahati, Assam, India. Contact No.: +918011002709, ORCID ID: 0000-0001-7007-2729
Email: arindam.dey@iitg.ac.in

* Corresponding author

Funding:
This research did not receive any specific grant from funding agencies like public, commercial or non-profit sectors.

Declarations of Interest
None

Finite Element Based Design and Analysis of Unpaved Roads over Difficult Subsoil: Sustainable Application of Geotextile Reinforcement to Attain Long-Term Performance

ABSTRACT

The performance and durability of an unpaved road depends on the strength of its individual components, i.e. aggregate layer and soil subgrade. For unpaved roads built over weak soil subgrades, the action of repetitive vehicular loading leads to permanent deformation in the form of rutting that gradually deteriorates the serviceability. In this study, initially, based on a coupled stress-deformation approach, a step-by-step design methodology of unreinforced unpaved road is developed by incorporating operational failure conditions. In order to avert the operational failures, geotextile layer introduced at the aggregate-subgrade interface is found to successfully reduce the stresses transferred to the subgrade. The usage of geotextile reinforcement is also found effective in reducing the required thickness of aggregate layer, as much as 50% in comparison to that required for unreinforced condition. Furthermore, finite element analysis of unpaved road under repetitive loading condition for different numbers of vehicle passes is conducted. When subjected to higher axle loads, rutting in unreinforced condition is observed to substantially increase with vehicle passes and even exceeding the serviceability criteria beyond certain cycles of loading. Geotextile layer at the aggregate-subgrade interface is found to successfully counteract the surface rutting. With the application of geotextiles of higher axial stiffness, not only rutting is conveniently controlled within the serviceability limit, the accumulation of rutting is also significantly arrested even for larger number of repetitive vehicular passes. Thus, through this FE-based analysis, the sustainable application of geotextile in unpaved road design and enhancing its performance under repetitive loading is successfully highlighted.

Keywords: Geotextile-reinforced unpaved roads, Finite element-based design, Operational conditions, Aggregate thickness, Rutting, Sustainable application

1. Introduction

According to global study, unpaved road comprises almost 80% to 85% of the world's road network [1]. In India [2] and USA [3, 4], 35%-50% of the road network is still unpaved. There are various types of unpaved roads, out of which gravel road or non-paved surface roads are the most common ones. Unpaved road structure consists of an aggregate layer directly placed over the natural soil subgrade [5, 6] without immediate application of any binder material such as asphalt or cement [7]. Unpaved roads carry low volume of traffic; thus, it is often economically viable to surface them with a bituminous seal if the average annual daily traffic (AADT) increases more than 300 [8]. However, in some specific cases, unpaved roads need to carry heavier vehicles such as in case of the access road to an industrial plant or a construction site, connecting or supply roads of goods from major village to nearby highway etc. Depending on unavailability of good quality material or site specific restrictions, unpaved roads are many a times constructed on weak or locally available soil having low bearing resistance. In such cases, unpaved road undergoes short-term or long-term deformation such as rutting, corrugation, potholes, washboard formations and surface degradation leading to dust emission [9-12]. In such cases, regular maintenance work such as replacing the unpaved road material (aggregate, soil subgrade) or incorporating soil stabilization technique (dynamic compaction, mixing of admixtures etc.) for the durability of the unpaved road becomes significant. However, regular maintenance work at regular intervals each time becomes highly cost incurring due to the involvement of man power and natural raw material extraction. Ground improvement techniques for subgrade strengthening induce more longevity to the unreinforced unpaved roads; yet such methods are significantly cost incurring processes and equipment. In this regard, use of geosynthetic as reinforcement in unpaved road structure has emerged as a sustainable and economical solution to the problem [13, 14]. In comparison to ground improvement techniques, laying of geotextiles at the aggregate-subgrade interface is a comparatively less time-consuming and less equipment-intensive process. Moreover, the performance life of the geotextiles is significantly high, which results in substantially lesser long-term maintenance costs. Hence, from the view of economic viability, application of geotextiles to construct reinforced unpaved roads has more long-term economic feasibility. However, to get a realistic assessment, a cost-benefit analysis needs to be done, which is beyond the purview of the present study.

Geosynthetics are the product of synthetic or naturally occurring polymeric material. The main applications of geosynthetics in areas such as civil, geotechnical, transportation, environmental etc. includes filtration, drainage, protection, separation, slope stabilization, soil reinforcement and stabilization [15-17]. There are various types of geosynthetics available commercially in planar or three-dimensional form such as geotextile, geogrids, geomembranes, geocomposites and geocells [18]. Commonly, out of all geosynthetics, geotextiles and geogrids are extensively used in unpaved roads [7, 19]. Generally, geosynthetic reinforcements are placed at the aggregate and subgrade interface to improve the unpaved road performance. Due to the tension membrane effect [20] and interlocking effect of geotextile and geogrid, respectively, the lateral movement of the aggregate materials is restrained, thereby improving the load distribution to the subgrade layer and ultimately increasing the bearing capacity of the subgrade layer [7, 14]. Earlier, researchers have worked on the application of geosynthetics in unpaved road. Giroud and Noiray [20] conducted two quasi-static analyses for the design of unpaved roads resting on a saturated cohesive subgrade with low permeability, in the absence and presence of a single layer geotextile reinforcement placed at the aggregate-subgrade interface. It was observed that due to the geotextile reinforcement, the aggregate thickness required to sustain the vehicular axle load can be reduced. Holtz and Sivagukan [21] continued the earlier work for different rut depths (additive of the maximum settlement occurring beneath the wheels and the maximum heaving occurring in between the wheels). It was found that for smaller rut depths, the geotextile primary worked as separator; however, at larger rut depths, the geotextile behaved as reinforcement. Bourdeau *et al.* [22] conducted an analytical study to critically examine the large-scale strip loading test of geotextile-reinforced unpaved roads on peat performed by Douglas and Kelly [23]. Through this study, the influence of geotextile anchorage and stiffness modulus on the soil-geotextile interaction and interface response was examined. The results from loading test suggested that there is no significant difference in the performance of unpaved roads with a woven or a non-woven geotextile or even a polyethylene film separator with different anchorage conditions and tensile moduli. Miligan *et al*. [24, 25] presented a new method for the design of unreinforced and reinforced unpaved roads under plane strain condition following the work by Giroud and Noiray [20] by considering the development of shear stresses at the subgrade-fill interface. The analysis demonstrated the role of reinforcement at smaller as well as larger rut depth. Tingle and Webster [26] conducted a full-scale test to validate the design criteria proposed by U.S. Army Corps of Engineers [27] for geotextile reinforced unpaved roads and modified the same for including a stiff biaxial geogrid reinforcement. From the tests conducted by

Tingle and Webster [26], comprising a moving load generated by 2000 passes of military trucks having single front axle weight of 4.76 tons and dual-tandem rear axle of weight 15 tons, it was observed that the bearing capacity factor for geotextile-reinforced unpaved road is unconservative as compared to the theoretical results [27]. Giroud and Han [28, 29] developed a generalized methodology to estimate the required thickness of the base course (aggregate layer) in reinforced unpaved roads with a single layer of geogrid placed at the aggregate-subgrade interface. Hufenus *et al*. [30] conducted full scale field test on the application of variation in geogrid stiffness on the reduction in rut depth formation of the unpaved road structure. Lyons and Fannin [31] highlighted the importance of proper choice and consistency of parameters while dealing with the semi-empirical design of unpaved roads. Perkins *et al*. [32] applied the mechanistic-empirical modeling methods previously developed for geosynthetic base-reinforced flexible pavements to reinforced unpaved roads. The model provides necessary information of rutting formation in unpaved road and the importance of excess pore pressure assessment on the stability of the structure. Calvarano *et al*. [14] conducted parametric study to give the limiting criteria of determining the base thickness of geogrid-reinforced unpaved roads. Calvarano *et al*. [16] conducted bi-dimensional finite element analysis, using FE software ABAQUS, to understand the performance of geogrid reinforced unpaved road under repeated loading. Han *et al*. [33] conducted cyclic shear test to the study reinforcing mechanism of geogrid in unbound granular base.

The application of geosynthetics in civil engineering construction is vast. However, the study of reinforcing mechanism of geotextiles and geogrids on controlling the individual and coupled deformation of components of an unpaved road structure are still limited. Moreover, the study of reinforcing mechanism of geosynthetics on reducing permanent deformation of unpaved road due to rutting is not well understood. Earlier researches on unpaved roads have been carried out considering the undrained cohesion as the only strength parameter of the subgrade [20, 21, 24, 25, 28, 29]. However, depending on the drainage state (undrained, partially drained or fully drained) of the soft soil subgrade, strength parameters are characterized by both cohesion (c) and angle of internal friction (φ). The consideration of conservative strength magnitude leads to over-estimated estimates of aggregate thickness which might not be practically required owing to subgrade strength actually available at the site.

Conventional limit equilibrium based analytical formulations consider the individual component (aggregate, subgrade) of the unpaved road to be non-deformable [20, 34]. However, in reality, different components of unpaved road undergo deformation even due to the operational aggregate placement and/or wheel loading. Considering all the factors, in this present study, finite element (FE) analysis of geotextile reinforced unpaved road constructed on cohesive-frictional (c-φ) soil subgrades is conducted. In this regard, the soil subgrade is considered to be weak to exhibit the full benefit of using geosynthetics. At first, FE analysis of unpaved road for quasi-static loading without reinforcement is carried out. It is observed that under different operational conditions, the individual layers of unpaved road undergo deformation. Further, the geosynthetic is introduced as a reinforcement at the aggregate-subgrade interface. It is observed that geosynthetics of various stiffness capture the stresses and strain generating in the unpaved road system with minimal application of ground improvement for subgrade strengthening. Further, an additional study of application of geosynthetic in reducing the thickness aggregate layer is also conducted. Later on, application of geosynthetic in reducing the rutting developed due to repetitive vehicular loading is discussed. It is observed with increase in stiffness of the geosynthetic, rutting in the unpaved road system is reduced. Further, it is noted that beyond a particular stiffness value, the rutting generated from particular number of vehicular loading cycles is completely arrested, thereby showing the benefits of using geosynthetic as reinforcement to construct an economical and sustainable unpaved road structure. In this regard, the novelty of the present work lies in the concept of using coupled stress-deformation approach to formulate a design principle of unpaved roads by considering its individual components as deformable bodies.

2. Quasi-Static Analysis of Unpaved Road

In this part of the study, the thickness of the aggregate layer is determined using the analytical formulations developed by Meena *et al*. [34] for unpaved roads resting on a generalized *c*-*φ* soil subgrade that is encountered more frequently in the field conditions. The developed expression is based on quasi-static analysis using limit equilibrium (LE) approach. Quasi-static analysis represents worst case scenario, wherein a vehicle is considered to be static for a significantly long time and as a result, there is a complete stress transfer through the interaction of the vehicle tire with the aggregate layer [20]. Fig. 1 represents the actual bi-directional pyramidal stress distribution that would occur beneath a quasi-static wheel load placed on the aggregate layer. Dual wheel vehicular axle load is considered in the present study [20], wherein each dual-wheel carries half of the axle-load ($P/2$). The load is transferred to the aggregate layer through the contact area of the dual wheel, whose equivalent dimensions are represented by m and n, respectively, thereby q_{eq} being the equivalent contact stress transferred at the tire-aggregate interface. Further, the generated contact stress on the surface of aggregate layer (q_{eq}) is assumed to follow a pyramidal stress distribution through the depth of the aggregate layer (H) and spread over a dispersed area at the aggregate-subgrade interface, having a dimension of m' x n'. It is to be further noted that at the aggregate-subgrade interface, the overburden stress due to the aggregate ($\gamma_{aggregate}H$) is omnipresent, and it gets added to the dispersed wheel stress to generate the total stress (q). Although the wheel stress distribution is a three-dimensional problem, this study considers only a two-dimensional dispersion scenario, with β being the load-dispersion angle. In the present study, it is considered that there is a constant and uniform flow of similar vehicle along the longitudinal section of the road. Furthermore, the wheels are assumed to always travel along the same section of the road such that every cross-section of the road receives the same magnitude of load and undergo same magnitudes of deformation [20]. Hence, the problem is considered as a plane-strain one, wherein every section has the same geometry and loading conditions. Under such scenario, in the absence of residual deformation along the longitudinal direction of the road, it is expected that the mechanical response of the roadway remains same at all the cross-sections [20], and equal strains are developed along the longitudinal direction of the road. Therefore, the quasi-static vehicular load analogically represents a strip load acting along the road. Hence, further, analyses for the present study are conducted within a two-dimensional plane-strain framework. The required aggregate thickness is determined by equating the stress generated at the aggregate-subgrade interface (Fig. 1) to the allowable subgrade strength. Equation 1 gives the final expression to determine the aggregate thickness (H) of unpaved road resting on *c*-*φ* soil subgrade.

$$\frac{P}{2(m+2H\tan\beta)(n+2H\tan\beta)} + \gamma_{aggregate}H = \frac{c_{subgrade}N_c + \gamma_{\text{aggregate}}HN_q + 0.5\gamma m' N_\gamma}{\text{FoS}} \tag{1}$$

where, P is the axle load, m and n are the equivalent contact dimension of the dual wheel, H is the thickness of the aggregate, γ is the unit weight of soil, $\gamma_{aggregate}$ is the unit weight of the aggregate, $c_{subgrade}$ is the cohesion in the subgrade, m' is the width of the distributed stress at the aggregate-subgrade interface, N_c, N_q and N_γ are the bearing capacity factors, and FoS is the factor of safety.

It is worth mentioning here that evaluation of California Bearing Ratio (CBR) is very essential for pavement design, and it has been the standard and pioneered practice in the design of unpaved roads to use CBR as an indicator of the undrained shear strength or undrained cohesion of soil [20]. However, the estimation of CBR disregards the frictional strength of soil material which, apart from cohesion, is another primary shear strength parameter. Thus, assessing the strength of cohesive-frictional soils through assessment of CBR remain conservative, thereby expectedly increasing the requirement of aggregate thickness of unpaved roads. Further, mere mention of CBR values do not allow distinguishing the types of soil; soils of two different characteristics can have a similar CBR. Hence, in such scenario, the intricate role of different types of soils in governing the behaviour of subgrades and unpaved roads remain elusive, which is supposed to have a critical role in controlling the generation of stress and deformations in the system. Hence, the primary aim of this study is to shift the perspective from standard CBR-based design to the coupled stress-deformation based design governed by the shear strength parameters (c and φ) of the geomaterials.

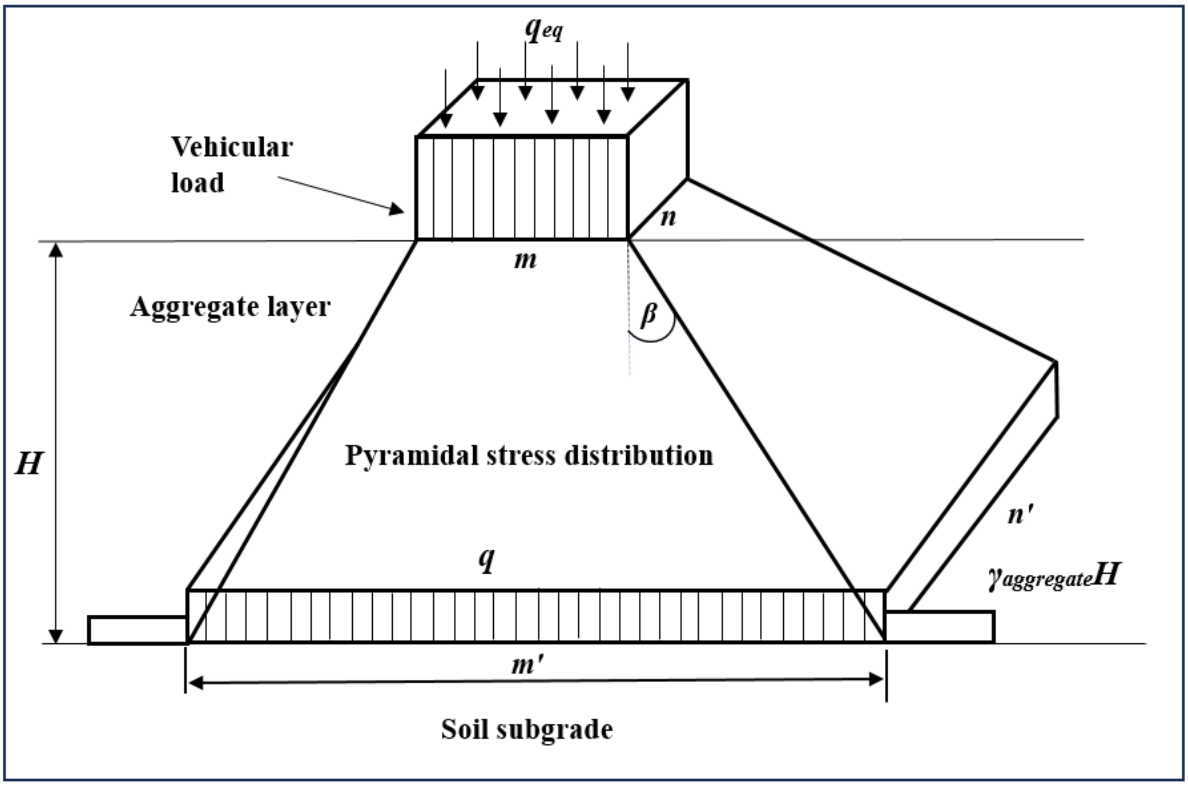

Fig. 1 Pyramidal stress distribution by aggregate layer on the subgrade interface

3. Numerical Methodology

The analytical formulations as shown in Equation 1 follows a stress-based approach, where the individual components of the unpaved road structure are considered to be non-deformable. However, in case of unpaved road built on weak or soft soil subgrade, deformation under different operational conditions becomes a guiding factor for the design [22, 35]. Different operational conditions include (i) failure or permanent deformation of weak subgrade layer due to the weight of stacked unbounded and poorly-graded coarse aggregate layer during their laying operation and (ii) failure within aggregate layer due to the stresses developed by vehicular loading. In this regard, and coupled stress-deformation based approach incorporating operational loading conditions becomes necessary to design sustainable and economic unpaved road system. In this study, a FE based design methodology of unpaved road structure subjected to quasi-static vehicular loading is discussed.

A finite element-based design of unpaved road resting on generalized *c-φ* soil subgrade is conducted. For the present research work, numerical modelling software PLAXIS 2D v2018 is used to design unpaved road system. Fig. 2 depicts a typical geometry of the unpaved road, comprising the overlying aggregate and underlying subgrade layers. The cross-section of the unpaved road is considered to be identical along the longitudinal section and hence plane-strain model is selected. 15-noded triangular elements are choose to model the soil layers and other aggregate volume, so that high quality stress-deformation results can be obtained. The thickness of the aggregate layer is initially designed from the analytical expression provided in Equation 1. The slope of the aggregate layer has been maintained to a value of 3H:1V or 4.5H:1V for higher axle load, to avoid any slope failure along the sides of the aggregate. Uniformly distributed vehicular load under tires are considered on the surface of the aggregate layers, over suitable contact width and axle width. Along the lateral boundaries of the subgrade layer, horizontal fixities are provided, while the bottom boundary of subgrade is fully fixed against both horizontal and vertical displacements.

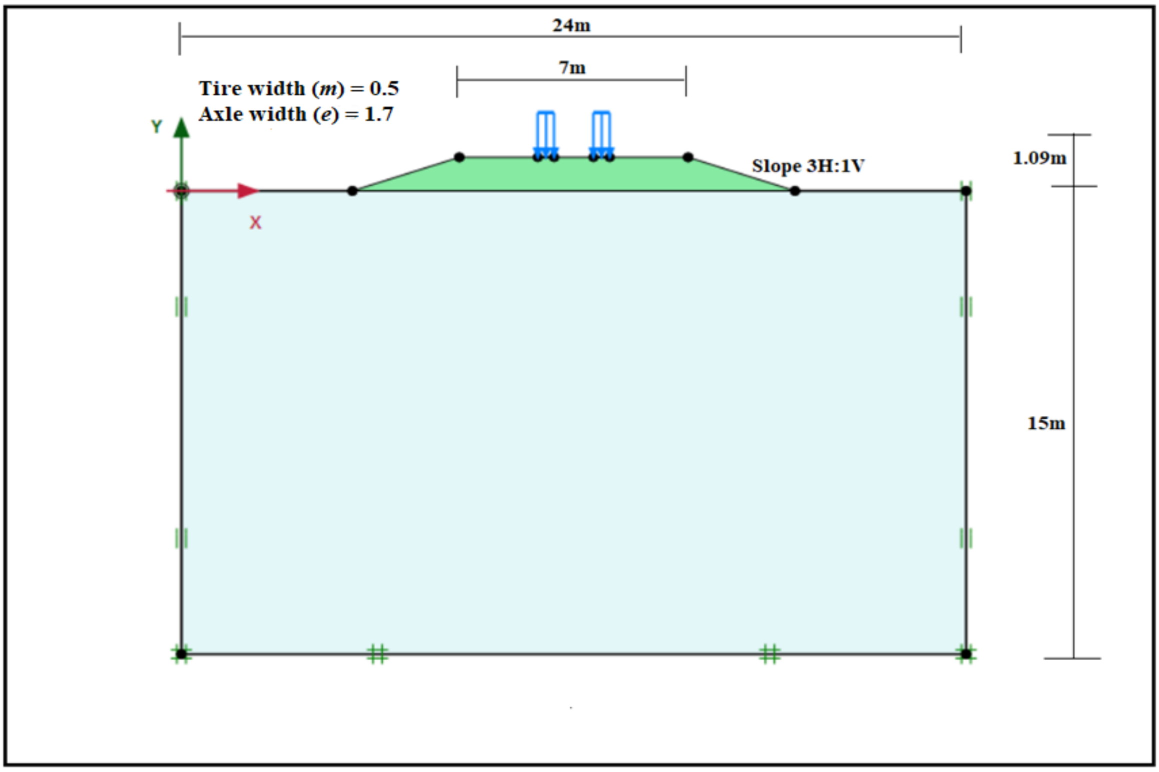

Fig. 2 Finite element model of unreinforced unpaved road

Both the subgrade and aggregate layer for the present study has been modelled using Mohr–Coulomb (M-C) model, which is a linear elastic – perfectly plastic model. This model allows elastic behaviour up to the yield limit, beyond which plastic flow occurs under constant stress. The Mohr-Coulomb yield point is defined by the friction angle of the material [36, 37]. Although the M-C model considers the variation of material strength with lateral confinement (wherein the material strength increases with stress level), it does not consider the variation of elastic modulus with stress levels [38]. The model is capable of capturing the hysteretic loading-unloading behaviour if plasticity occurs, i.e. if the yield stress level is reached [39, 40]. The loading, unloading and reloading modulus remain constant (equal to chosen Young's modulus) for each cycle of stresses. Each cycle of loading-unloading is characterized by a residual strain or residual deformation, with a portion of total strain being recovered due to the elastic unloading. Hence, in case of repetitive loading, the M-C model is capable of producing accumulative settlement, provided that at each loading and reloading cycles, the yield stress is attained. In such case, for repetitive loading, the accumulation of settlement would be noticed after each loading cycle, as depicted in later parts of the present study.

The constitutive behaviour of Mohr – Coulomb model is controlled by five input parameters, soil elasticity and stiffness represented by Young's modulus (E) and Poisson's ratio (v), and angle of internal friction (φ), cohesion (c) and angle of dilatancy (ψ) for soil plasticity [41]. For the present study, dilatancy is not considered. The strength parameters of subgrade and aggregate layer are considered on the lower side so that the deformations developed in the unpaved road system under operational conditions can be exclusively exhibited. In Table 1, the typical model parameters used in the present study are listed that are chosen as available in the earlier literature [34, 42]. These are some typical values of the parameters that falls within the wide range of material parameters that could be reasonably encountered in the construction of such unbounded roads. For the subgrade layer and aggregate layers, the unit weight (γ) is kept same owing to the fact that the unit weight of soil and locally available aggregates are mostly similar and that slight variations in this parameter does not significantly affect the deformation response of the unpaved road system [34]. Two different vehicular axle loads 80 kN and 190 kN are used in this study for quasi-static and repetitive vehicular loading analyses.

Table 1 Typical material properties adopted in the finite element analyses

	Subgrade	**Aggregate**
Soil model	Mohr-Coulomb	Mohr-Coulomb
Unit weight (γ)	19 kN/m^3	19 kN/m^3
Young's modulus (E)	20 MPa	60 MPa
Poisson's ratio (v)	0.4	0.3

A mesh convergence study has been carried out for a particular model to identify the sensitivity of the FE model to the variation in mesh size. In Plaxis 2D, finite element meshes of various element sizes can be generated by taking into account the soil stratigraphy as well as all objects, loads and boundary conditions. It is obtained from the output results that for 'medium' mesh size, the convergence has been achieved. Fig. 3 represents the outcome of the mesh convergence study conducted for the model. In areas of large stress concentrations, local mesh refinement has been also provided (e.g., aggregate-subgrade interface, corners of the aggregate layer, etc.). Fig. 4

shows the model after mesh refinement, with an average element size of 0.07727 m; the same element size is used in all other FE models reported in the manuscript.

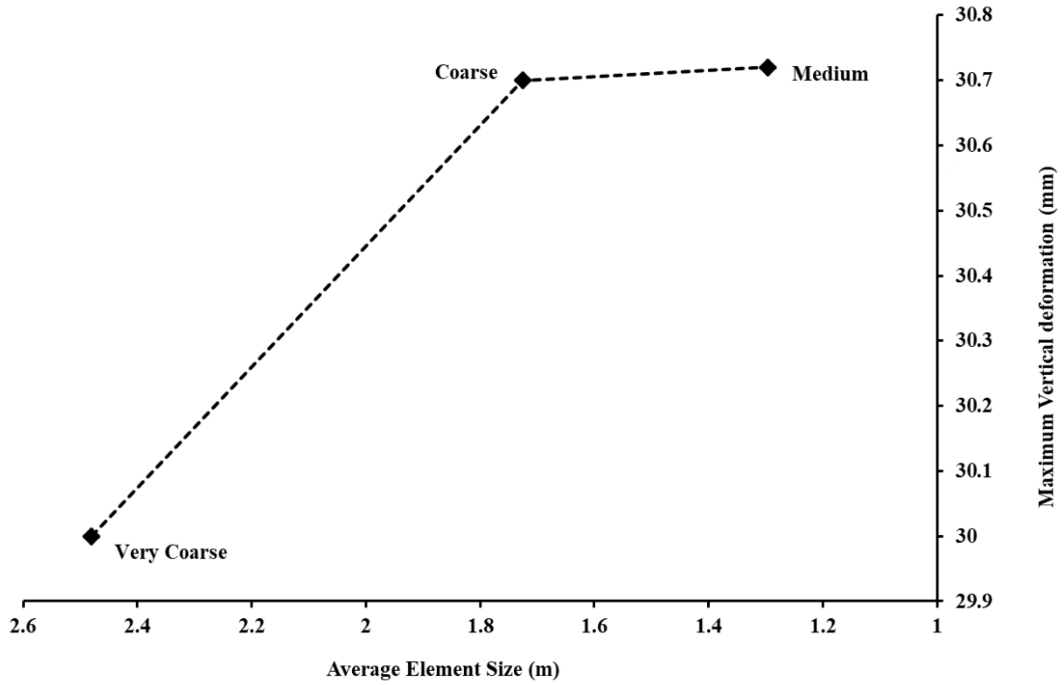

Fig. 3 Optimal mesh size determination from mesh convergence study

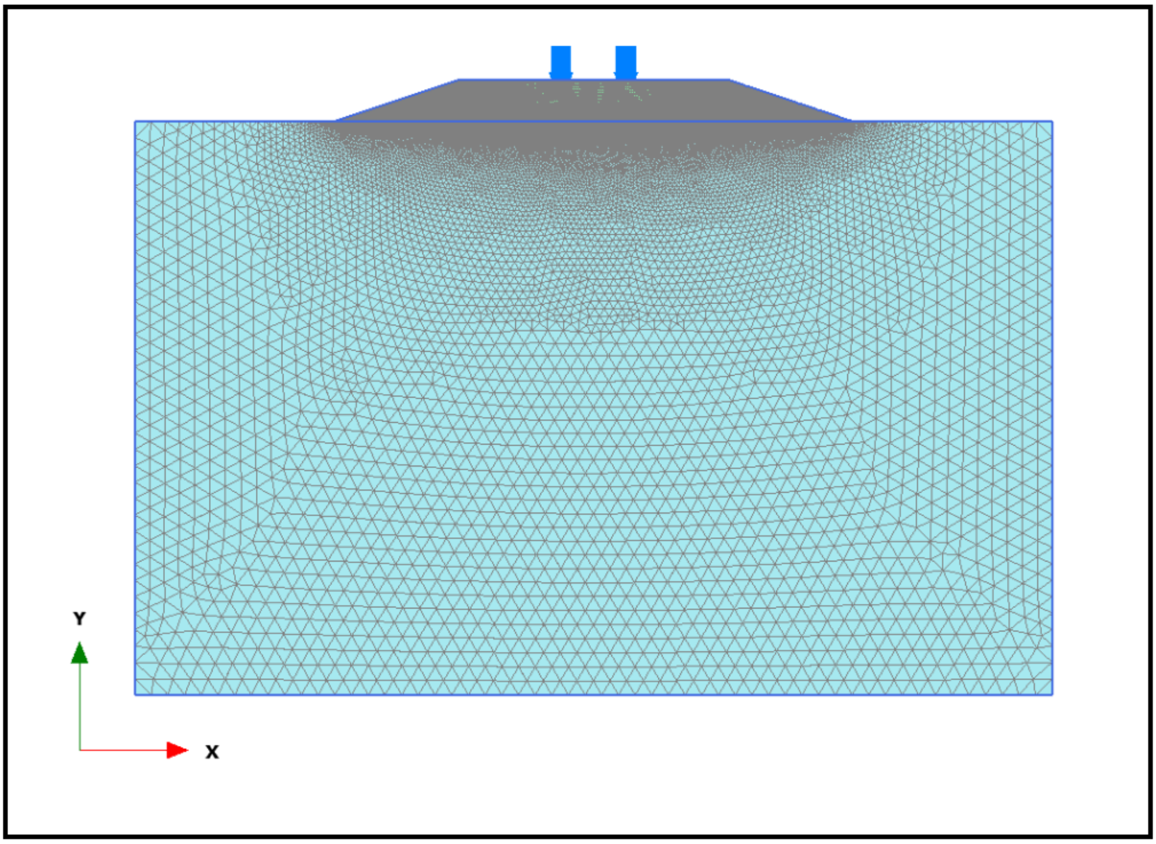

Fig. 4 FE model of unpaved road generated after refined meshing

To understand the efficiency of the coupled stress-deformation based design approach and the constitutive behaviour of the individual component of the unpaved road, a validation study has been carried out. The FE model of the unpaved road, comprises of two layers (aggregate layer overlying the subgrade layer) with a strip vehicular loading (representing the quasi-static vehicular load) over the aggregate layer. The experimental problem reported by Ghosh and Kumar [43] on surface strip footings resting on two layered media is analogically considered for the validation work. Out of all experiments conducted in the study, footing width (*B*) of 50 mm, center-to-center spacing of the footing (*S*) as 3.0*B* (= 150 mm), and thickness of the top layer (*D*) being equal to 1.0*B* (= 50 mm) is considered of the validation work. The angle of friction of the top (φ_1) and bottom layer (φ_2) were 32.6º and 38.9º, respectively. A FE model is developed considering all the necessary information related to the footing material, soil properties, loading conditions and measurement points. Fig. 5 shows the FE model utilized for the validation study. To find out the settlement values, nodes are selected on both side and at the centre of the footing. The selection of the nodes is based on the position of the dial gauges used in the experimental set up. For the selected nodes, the data obtained for settlement and load is averaged and put in a single plot

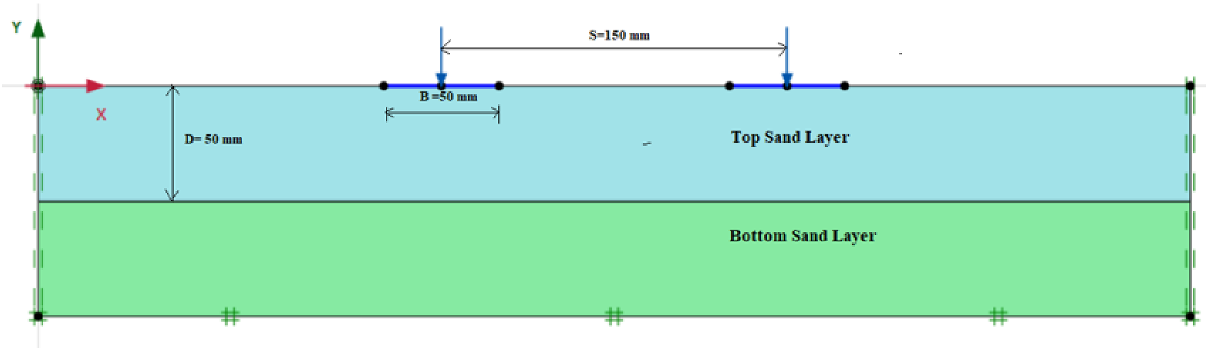

Fig. 5 FE model for the validation study

The output results of the FE analysis, in the form of load-settlement response, are compared to that obtained from the experimental observation (Fig. 6). The load settlement responses exhibited a reasonable agreement; for a maximum settlement of 6 mm, the ultimate load obtained from the experimental and numerical exercise is 33 kg and 35 kg, respectively. A minor dissimilarity can be noted between experimental and FE results (with an average deviation of 5-8% for most part of the plot), which is possibly due to the idealization of the stiffness of experimental sand bed being constant in Mohr-Coulomb constitutive model, whereas the actual experimental programs generally reflect a pressure-dependent stiffness. However, such minor dissimilarity remains existent and are well within the tolerable limit (<10%). Thus, from the study, it can be well inferred that the constitutive behaviour of FE model for the closely spaced loading resting two layered soils successfully validate the experimental results; hence, the developed FE modelling approach can be suitably considered in the rest of the study.

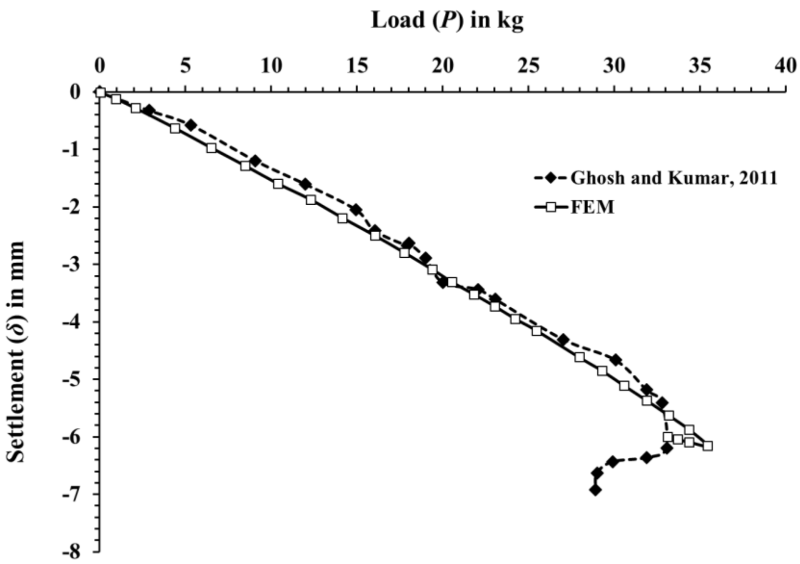

Fig. 6 Comparative of the load-settlement response between the experimental and FE results

4. Coupled Stress-Deformation based Design Methodology for Unpaved Roads

4.1 Operational failure conditions and limiting cohesion

The analytical expression expressed in Equation 1 considered the aggregate and subgrade layer to be non-deformable. However, in reality, both the subgrade and the aggregate are deformable systems. For weak and soft soil subgrade, the subgrade might not provide the bearing resistance during the laying process of stacked unbounded aggregate. This would be manifested by the subsidence of the aggregate within the subgrade layer, thereby This leading to a loss in design thickness followed by additional aggregate placing, and incurring higher expenditures of material and cost. Furthermore, in the absence of fine binding material in the cluster voids, aggregate can undergo punching failure that is prevalent under the vehicular loading at the edges of the tire contacts. These two stated failures constitute the operational failure during the construction and service life of the unpaved road, that is not incorporated in the analytical solutions. In this regard, the strength parameters of the aggregate and soil subgrade needs to be improved to counteract such operational failures. The expressions for the minimum cohesion required individually by the subgrade and aggregate are determined from limit analysis. The expressions to assess minimum cohesion are incorporated to propose the coupled stress-deformation based approach for FE model of unpaved roads.

4.1.1 Expression for limiting cohesion in subgrade layer required to sustain aggregate loading

The subgrade should be strong enough for sustaining the aggregate load during its placement. Hence, following Terzaghi's bearing capacity formulation for an analogous surface strip load resting on supporting soil [44], the expression for minimum cohesion required by subgrade under operational condition has been developed by equating the aggregate stress ($\gamma_{aggregate}H$) to the allowable bearing capacity of the subgrade. The same is expressed as follows:

$$\gamma_{aggregate} H = \frac{c_{subgrade,\min} N_c + 0.5\gamma m' N_\gamma}{\text{FoS}} \qquad (2)$$

where, $c_{subgrade,\min}$ is the minimum cohesion required in soil subgrade, and rest of the parameters are same as described in Equation (1).

4.1.2 Expression for limiting cohesion in aggregate layer required to sustain quasi-static vehicular loading

The aggregate layer under quasi-static loading might experience punching shear failure from the concentrated stresses developed at the siders of the wheel. In such case, the stress concentration under edges of the tire contacts should be dispersed to a magnitude lower than the allowable bearing capacity of the aggregate alone. Hence, following Terzaghi's bearing capacity formulation for a surface strip load resting on supporting soil [44], the expression for minimum cohesion required by the aggregate ($c_{aggegate,\min}$) under operational condition can be expressed as

$$\frac{P}{2mn} = q_{eq} = \frac{c_{aggregate,\min} N_c + 0.5\gamma_{aggregate} m' N_\gamma}{\text{FoS}} \quad (3)$$

where, $c_{aggregate,\min}$ is the limiting cohesion required to prevent punching shear failure in the aggregate layer due to the imposed quasi-static vehicular loading. The corresponding bearing capacity factors are to be determined based on the friction angle of the aggregate material.

4.1.3 Additional cohesion requirement of subgrade considering deformability of aggregate and subgrade

In the previous sub-sections, separate expressions to determine minimum cohesion required by the subgrade and aggregate to ensure their individual operational stability against failure are produced. However, in practical scenario, the stress-deformation mechanism of the unpaved road system will be coupled and the subgrade would be a deformable medium; thereby, the stability of individual layers would be affected by the secondary stress transfers through stress-deformation interaction between the layers. Since under vehicular load the aggregate layer is already ensured to be stable, further failure in this layer under operational condition can only be triggered because of the deformable subgrade. Hence, in such situation, the cohesion of the subgrade needs to be further modified to arrive at a minimum value ($c_{sagg,\min}$) that would render the subgrade enough bearing strength to sustain the overall imposed stress, inclusive of the secondary stresses. In the next section, implementation of such expressions is discussed. Such improvement in strength of the subgrade is possible by adopting proper ground improvement techniques, wherever necessary, although the choice of the ground improvement techniques is beyond the scope of the present study.

4.2 Design Methodology for Unreinforced Unpaved Road Design

Following are the step-by-step design procedure of unreinforced unpaved road structure based on coupled stress-deformation based approach.

Step 1. Make a preliminary assessment of the required aggregate thickness (H) based on Equation 1.

Step 2. Develop the FE model in PLAXIS 2D using aggregate thickness assessed in Step 1. The side slopes of the aggregate layer are maintained to 3H:1V or any other flatter gradient to ensure that no side-slope failure is evident. The shear parameters ($c_{subgrade}$, $\varphi_{subgrade;}$ and $\varphi_{aggregate}$) for subgrade and aggregate layers is to be kept same as that used in the analytical expression used for assessing the aggregate thickness [34]. The values of other model parameters such as modulus of elasticity (E), Poisson's ratio (v), unit weight (γ) and initial void ratio (e_{init}) are adopted as per field specifications.

Step 3. The simulation of the FE model developed in Step 2 is undertaken to investigate the operational instability of the subgrade solely due to aggregate loading. If the operational stability is not jeopardized, consider $c_{subgrade,\min}=c_{subgrade}$ and continue to Step 6. If the FE model exhibits stress-based failure in the subgrade, continue to Step 4.

Step 4. Assess the limiting magnitude of cohesion ($c_{subgrade,\min}$) required in the subgrade layer (as per Equation 2) to sustain the operational aggregate loading.

Step 5. Using the $c_{subgrade,min}$ value obtained in Step 4, analyse the FE model developed in Step 2 to ascertain the operational stability of the subgrade under aggregate loading. If the subgrade remains stable under the aggregate load, continue to Step 6. If the subgrade still portrays failure, repeat Step 4 to re-estimate $c_{subgrade,min}$ with higher FoS.

Step 6. Reform the FE model by incorporating $c_{subgrade,min}$ as the cohesive strength parameter for the subgrade (obtained in Step 5) over and above the friction strength parameter of the subgrade ($\varphi_{subgrade}$). Investigate whether the aggregate layer (with strength parameter adopted in Step 1 or Step 2) is operationally stable and able to sustain the punching stress concentration imposed by the quasi-static vehicular load.

Step 7. If operational stability of aggregate layer is ensured, the design of unpaved road is deemed complete with $\varphi_{subgrade}$ and $c_{subgrade,\min}$ as the shear strength parameters for the subgrade, and $\varphi_{aggregate}$ as the shear strength parameter for the aggregate.

Step 8. If the aggregate fails under the imposed vehicular load, determine the minimum value of cohesion required ($c_{aggregate,\min}$) in the aggregate using Equation 3.

Step 9. Analyse the reformed FE model developed in Step 6 (already having $\varphi_{subgrade}$, $c_{subgrade,\min}$ and $\varphi_{aggregate}$) by incorporating $c_{aggregate,\min}$ as limiting aggregate cohesion to reassess its operational stability.

Step 10. If the aggregate still exhibits operational instability, considering a higher FoS. Further, proceed to Step 9 to include the re-estimated $c_{aggregate,\min}$ in the reformed FE model that is already incorporating the $\varphi_{subgrade}$, $c_{subgrade,\min}$ and $\varphi_{aggregate}$ (from Step 6). If the reformed FE model with higher magnitude of $c_{aggregate,\min}$ in aggregate layer exhibits operational stability, proceed to Step 11; else, repeat Step 10 again by heuristically and iteratively enhancing $c_{aggregate,min}$ to a higher value.

Step 11. If the aggregate does not exhibit stress-based failure under imposed load and that the operational stability of the aggregate is ensured, the strength parameters of unpaved road system is finalized to

$\varphi_{subgrade}$ and $c_{subgrade,\min}$ as the shear strength parameters for the subgrade, along with $\varphi_{aggregate}$ and $c_{aggregate,\min}$ as the shear strength parameter for the aggregate. Even after achieving operational stability, it is necessary to check whether the reformed FE model exhibits failure in the subgrade due to the secondary stresses generated in the subgrade for simultaneous aggregate and vehicular loading. The unpaved road system is further checked for failure under secondary stresses.

Step 12. If no secondary stress-based failure is noticed, the design of unpaved road system is deemed complete with the strength parameters finalized and mentioned in Step 10.

Step 13. Any instability in the subgrade arising due to the secondary stresses (as in Step 11) can be tackled by heuristically and iteratively increasing the value of $c_{subgrade,\min}$ to a modified higher value ($c_{sagg,\min}$).

Step 14. The FE model is reanalysed with $c_{sagg,\min}$ as subgrade cohesion to reconfirm the stability of the system.

Step 15. If the stability against secondary stresses is achieved, the design of unpaved roads is deemed complete with the strength parameters of unpaved road system is finalized to $\varphi_{subgrade}$ and $c_{sagg,\min}$ as the shear strength parameters for the subgrade, along with $\varphi_{aggregate}$ and $c_{aggregate,\min}$ as the shear strength parameter for the aggregate. If the stability is yet to be achieved, repeat from Step 13.

For easy visualization, Fig. 7 exhibits the developed algorithm in the form of a flowchart.

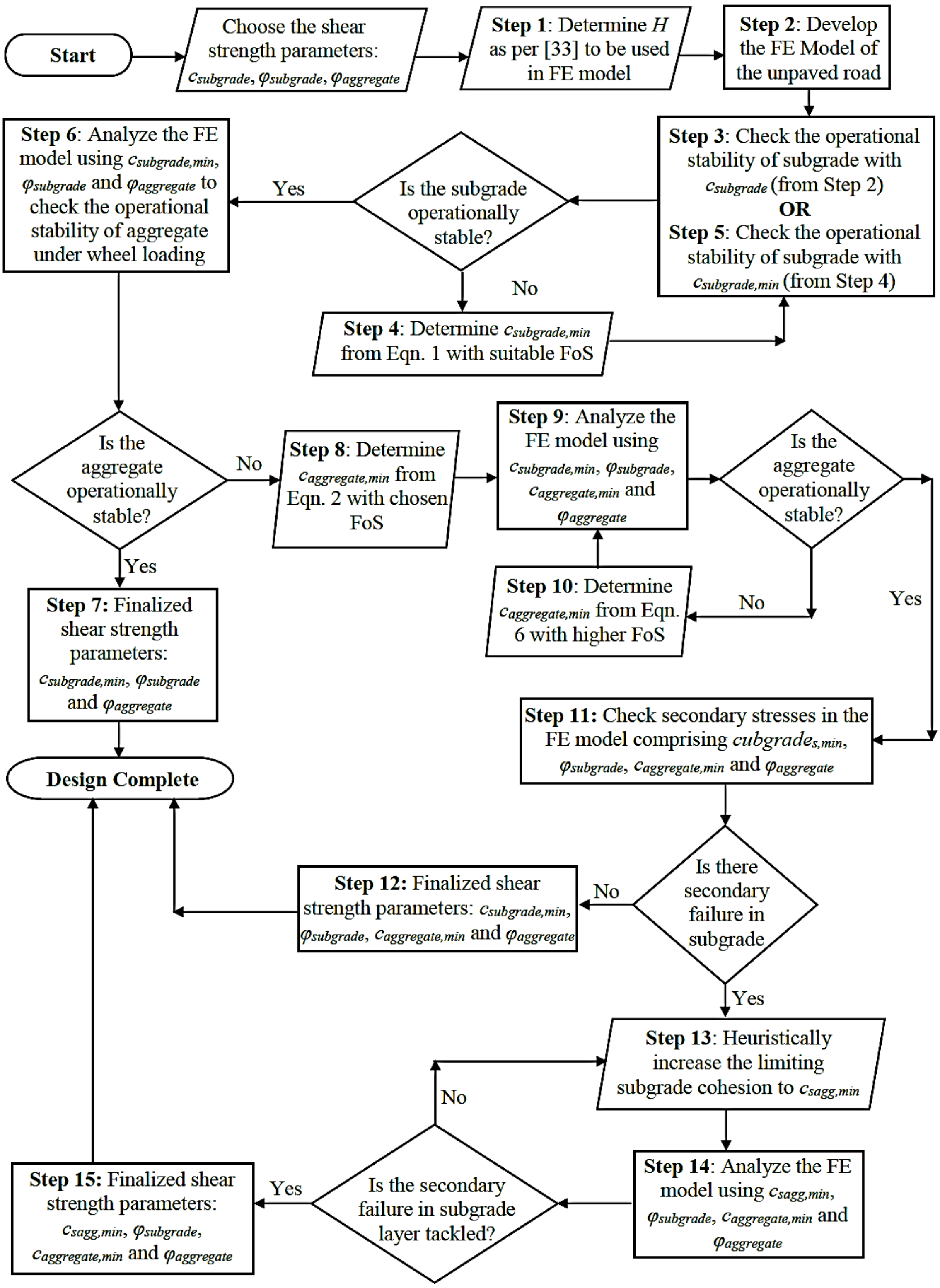

Fig. 7 Flowchart depicting the step-by-step design of unreinforced unpaved road

4.3 Design Methodology for Reinforced Unpaved Road

4.3.1 Quasi-static loading condition

In the previous part of the study, it is understood that unreinforced unpaved road built on soft soil subgrade is susceptible to deformation under operational conditions. To counteract such problems, ground improvement techniques need to be implemented to ensure stability of the unpaved road system. However, traditional ground improvement techniques are costly and require space and lots of manpower (soil replacement, compaction etc). Use of geotextile as reinforcement is an economic and sustainable solution to the problem. Geotextiles are planar members that can sustain and induce tensile force within the compressible soil. In Plaxis 2D, two types geosynthetic material comprising 3-noded and 5-noded elements are available. The selection of type geosynthetic element depends on the type of soil element provided in the project properties section. For the present study, 15-noded soil element is provided and 5-noded geosynthetic element is used. The geosynthetic element is represented by elastic and isotropic material behavior. For an elastic geotextile, the main material property is its axial stiffness (EA). The axial stiffness value was varied between 200-1000 kN/m (within the range for woven geotextiles available in practice for road construction projects) to understand the benefit imparted by geotextiles with different stiffness values [20, 33]. For proper bonding between the geosynthetic and the surrounding soil, interfaces are provided on both sides of the geosynthetic. It can be noted that the geosynthetic is placed at the interface of aggregate and subgrade. Hence, in the numerical model, two interfaces are created; one between aggregate and geosynthetic (i.e. above the geosynthetic) and the other between geosynthetic and subgrade (i.e below the geosynthetic). R_{inter} governs the amount of strength parameter to be considered for the interface; a value of 0 (zero) signifies interface to be smooth and full slippage is allowed, while a value of 1 (one) emulates perfect bonding through a rough interface where no slippage is allowed. In the present study, the latter (i.e. R_{inter} = 1) is adopted considering a perfect bonding between the materials. Under such condition, the strength parameter of the interface is chosen to be the same as that of the adjacent soil. In this case, the interface above the geosynthetic inadvertently uses the strength properties of the aggregate while the one below the geosynthetic uses the strength parameters of the subgrade.

As discussed in Section 4.2 for unreinforced unpaved roads, in Steps 3-5, the subgrade is considered failing under aggregate loading. Further, in Step 11, the subgrade again is considered for failure due to the secondary stresses generated by simultaneous aggregate and vehicular loading. Instead of adopting a conventional ground improvement technique to induce modified strength parameters for subgrade and aggregate to ensure the stability of unpaved road, incorporation of geotextile layer is considered and the model is analysed in the corresponding steps for different operational conditions. However, yet there might be some cases of extremely weak subgrade wherein even after incorporating geotextiles of higher stiffness, the subgrade might show signs of impending failure; in such cases, some ground improvement technique needs to be inadvertently adopted to ensure stability of the reinforced unpaved road system.

4.3.2 Repeated Loading condition

In the previous section, FE analyses were adopted to conduct quasi–static analysis for designing and assessing the performance of unpaved roads. Although quasi-static analysis represents a worst-case scenario, in actual field scenario, load repetition effect due to vehicular passages comes into picture. Therefore, a FE-based study is conducted to decipher the effect of vehicular load repetition on the behaviour of unreinforced and reinforced unpaved road. The problem is tackled as a quasi-dynamic problem. In this case, the actual time-dependent spatial movement of the vehicle is represented in terms of the axle load repetitions at specific intervals of time. In such consideration, the main parameters of load repetition were considered as the vehicle axle load (*P*), number of load passes (*N*) and time interval of two consecutive passes (Δ*t*). In the present problem, the quasi-dynamic load is applied through dynamic load multipliers having the axle load as the amplitude repeated at regular time interval of 0.4s. Fig. 8 shows the sequence of input dynamic load, expressed through a triangular waveform to provide a representative sequence of vehicles with similar axle load passing a section of a road at regular time intervals. The rising arm of the triangular input (over a time interval of 0.1 s) signifies the vehicle is approaching at a road section, following which it reaches a maximum magnitude equal to the axle load of the vehicle, and subsequently followed by the falling triangular arm over a time interval of 0.1 s) signifying the vehicle leaving the unpaved road section. Hence, the overall time duration of the passage of vehicle over a particular section is 0.2 s.

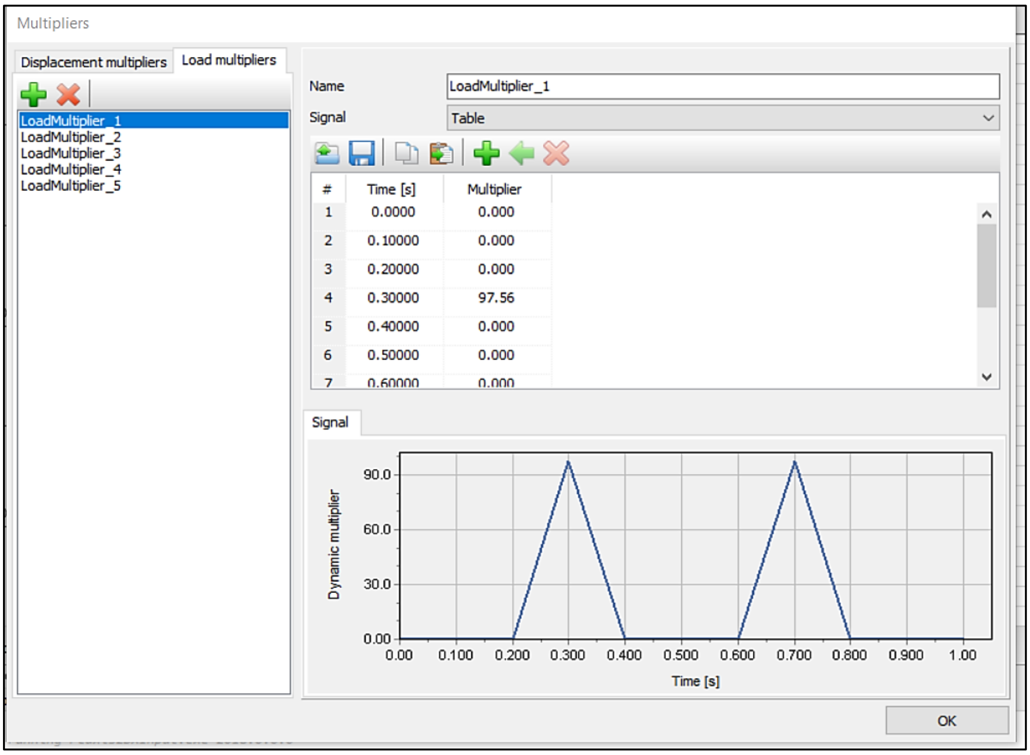

Fig. 8 Triangular load distribution signifying the quasi-dynamic vehicular load repetition

In this study, influence of repetitive loading conditions on unpaved road structure are investigated for both unreinforced and reinforced scenarios. The development of FE model of unpaved road is similar to the quasi-static loading condition discussed in a preceding section. The main difference is the input of the repeated loading that is described in the previous paragraph. Initially the response of unreinforced FE model of unpaved road is observed under repetitive loading for a particular material model parameter. If the unreinforced unpaved model shows signs of failure due to the rutting at the surface of the aggregate layer due to repeated loading, a geotextile layer is introduced to develop the reinforced model of unpaved road and subsequently analysed.

5.0 Results and Discussion

This section gives the FE output results of unreinforced as well as reinforced unpaved road under quasi-static and repeated loading condition.

5.1 Quasi-Static loading

In this section, finite element-based design of an unpaved road system under quasi-static loading condition is discussed. The parametric values for the analysis of the parent model considered herein are P = 80 kN, P_c = 600 kPa, m = 0.37 m, $c_{subgrade}$ = 1 kPa, $\varphi_{subgrade}$ = 5° and $\varphi_{aggregate}$ = 25° and FoS = 1. In the parent model, strength properties of subgrade and aggregate layers are considered in such a way that the individual layers undergo deformation and the minimum cohesion-based design is illustrated through the FE-based design methodology. Later on, the benefit of incorporating geosynthetics in the parent model are exhibited.

5.1.1 Outcomes from a typical FE-based simulation for unreinforced unpaved road

As discussed in Section 4.2, a step-by-step design methodology of unpaved road structure without geosynthetic reinforcement is conducted. The outcome of the design is as follows:

- **Step 1**: Based on the parametric data and following Equation 1 (with FoS=1), the thickness of aggregate layer (H) is preliminarily assessed to be 0.79 m.
- **Step 2**: Fig. 9 shows the FE model developed with the thickness of aggregate layer obtained in Step 1. The material properties of the model are kept as same as mentioned above and the side slopes of the aggregate layer are maintained to 3H:1V.

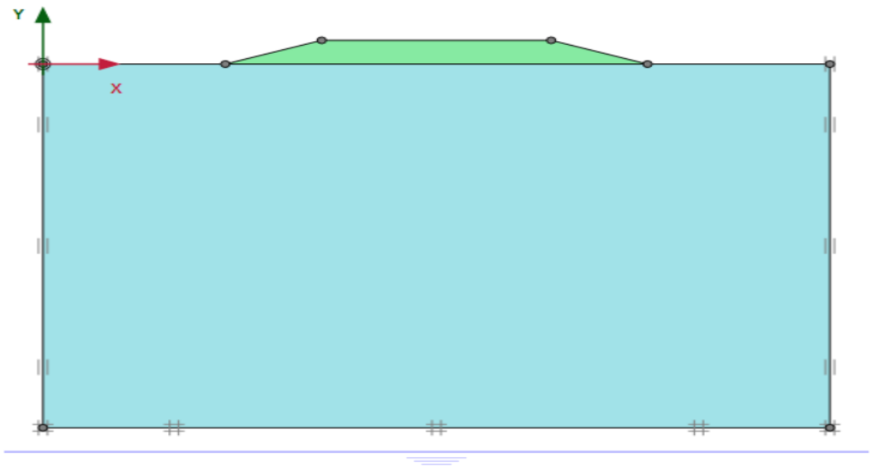

Fig. 9 FE model of unpaved road with subgrade subjected to aggregate loading

- **Step 3**: The operational stability of the subgrade is checked under the aggregate loading. Fig. 10 shows that under aggregate loading, significant deviatoric strains have developed as manifested by the slip lines propagating through the aggregate layer to the subgrade layer. The observation indicates that the subgrade is not sufficiently strong to bear the aggregate loading and that it fails even due to the laying of the aggregate, thereby necessitating enhancement in its strength properties.

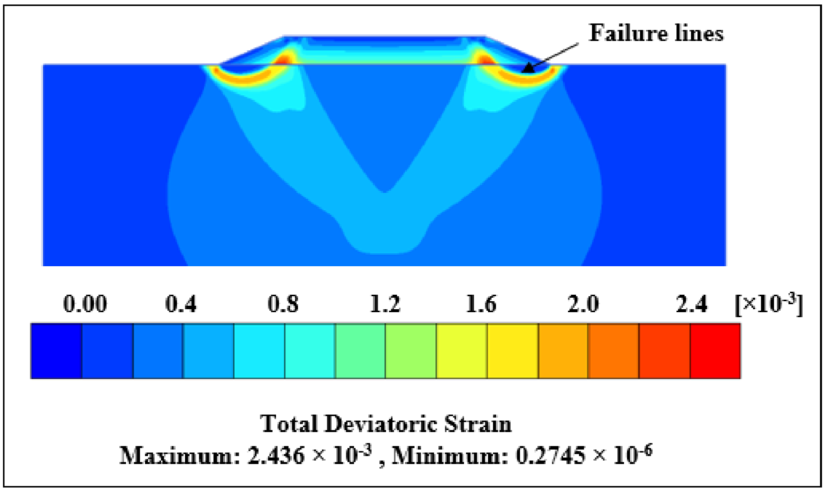

Fig. 10 Total deviatoric strain diagram of subgrade subjected to aggregate loading considering basic parametric

- **Step 4**: Following Equation 2 and considering FoS=1, the minimum cohesion ($c_{subgrade,min}$) required in the subgrade layer to sustain the aggregate loading is assessed to be 1.82 kPa, which is more than the previously considered value of $c_{subgrade}$ = 1 kPa.
- **Step 5**: $c_{subgrade,min}$ = 1.82 kPa is used in the FE model and the operational stability of the subgrade is rechecked. Fig. 10 shows the total deviatoric strain diagram and it can be noted that the strains are well captured and restricted within the aggregate layer. These observations conclusively indicated that with improved strength parameters, subgrade is capable of bearing the aggregate load. Hence, $c_{subgrade,min}$ = 1.82 kPa is used in the subsequent analyses.

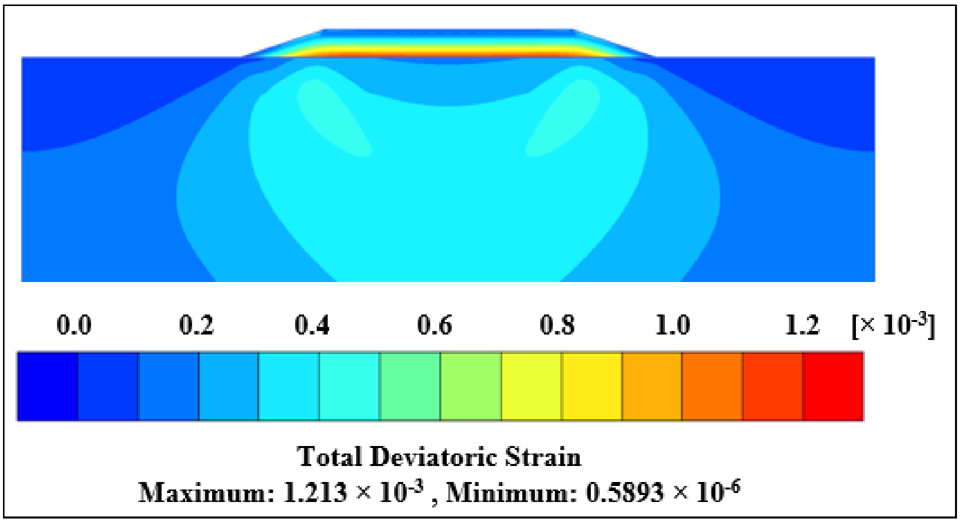

Fig. 11 Total deviatoric strain diagram of subgrade subjected to aggregate loading considering the improved strength parameter of subgrade

- **Step 6**: With the quasi-static vehicular load applied on to the aggregate layer resting on the reformed subgrade (as shown in Fig. 12), the FE model is analysed for the operational stability of aggregate layer.

It is observed that under vehicular load, the FE model simulation exhibited failure. Fig. 13 shows the total deviatoric strain diagram, wherein it is noted that the strains are heavily concentrated within the aggregate layer and maximum at and around the edges of the wheels. This indicates the development of punching shear failure mechanism within the aggregate layer due to the imposed wheel load. Based on the output results, it is understood that the strength parameters of the chosen aggregate are insufficient to prevent failure in aggregate layer due to the vehicular load. Hence, there is a necessity to improve the aggregate strength.

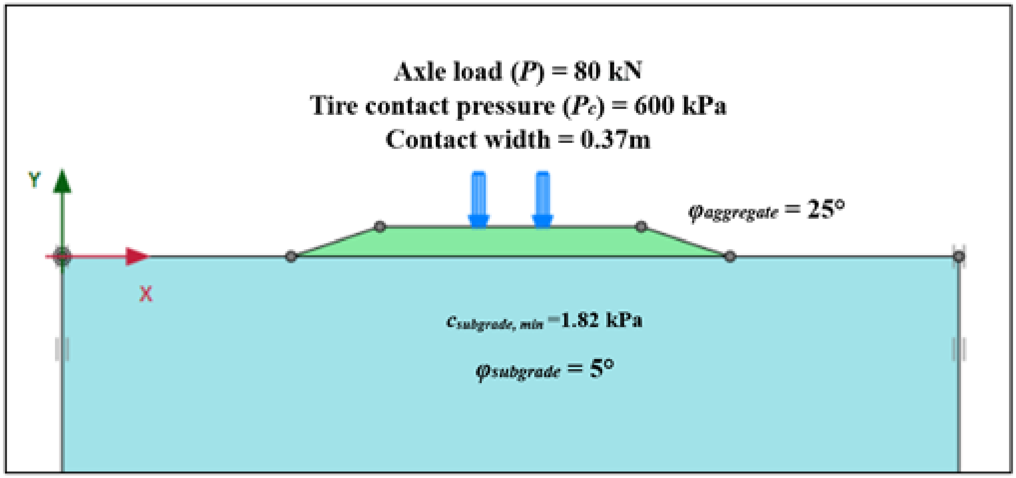

Fig. 12 FE model of unreinforced unpaved road subjected to vehicular load

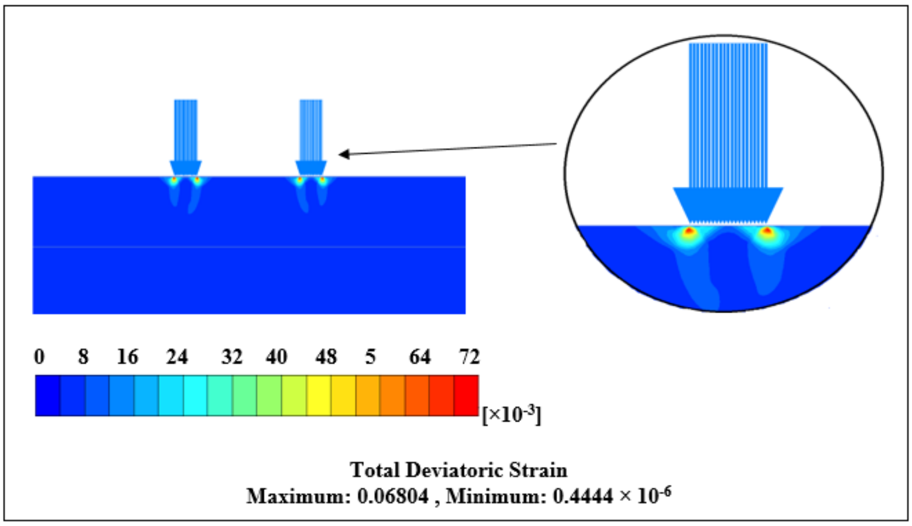

Fig. 13 Total deviatoric strain diagram of unreinforced unpaved road with basic strength parameters of aggregate layer and subjected to vehicular load

- **Step 7**: As the aggregate is not operationally stable, the final shear strength parameters are not achieved, and the design is progressed to Step 8.
- **Step 8**: Following Equation 3 and with FoS=1, the strength parameter of the aggregate layer is further increased and the minimum value of cohesion required in the aggregate layer ($c_{aggregate,\min}$) is determined to be 15.56 kPa.

- **Step 9**: Subjected to quasi-static vehicular loading, the FE model developed in Step 6 is further analysed with increased cohesion of aggregate ($c_{aggregate,\min}$). However, even with the enhanced strength parameter of the aggregate, the FE model again exhibited further failure. It is observed from Fig. 14 that as the failure in the aggregate layer is arrested by increasing the strength within the layer, additional secondary stresses are getting transmitted towards the subgrade, thereby leading to the failure of unpaved road system. Incremental deviatoric strain diagram depicts the development of the slip lines within the subgrade, thereby indicating the bearing capacity failure of the subgrade due to the migration of strain concentration from the aggregate to the subgrade through the interface.

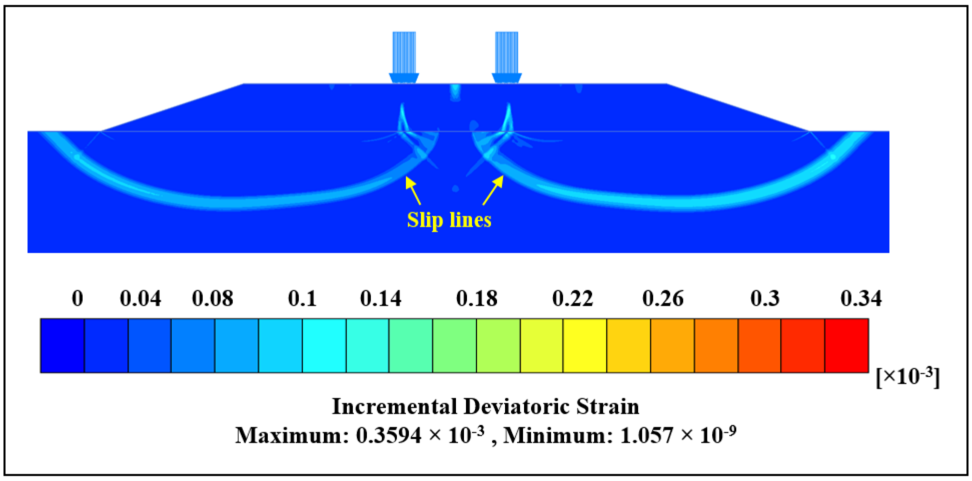

Fig. 14 Response of subgrade subjected to vehicle loading considering the improved strength parameter of aggregate in terms of incremental deviatoric strain developed in the system

- **Step 10**: Based on Equation 3, the cohesion of aggregate layer is further enhanced to a value of 24.01 kPa, by considering a higher FoS value of 1.5.
- **Step 11**: However, even with the enhanced aggregate strength, the unpaved road system still undergoes failure. Fig. 15 shows the plastic point or potential failure points developed in the subgrade layer due to the stress-transfer from aggregate to subgrade layer under quasi-static vehicular load. The development of plastic points is an indicator of the distribution of potential failure points that stem from the comparative of the stress distribution and strength at different locations within the subgrade Thus, it is understood that the strength of the subgrade layer needs further enhancement to tackle the developed secondary stresses.

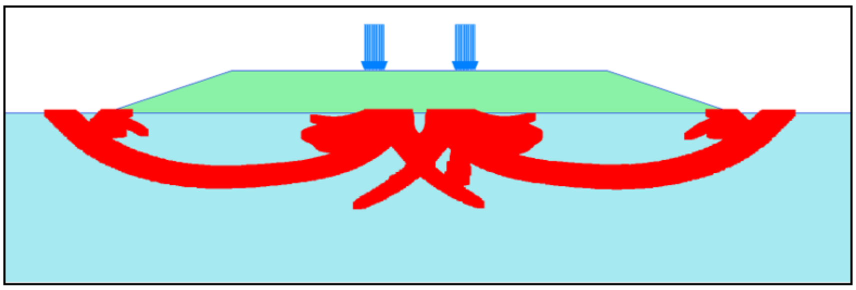

Fig. 15 Plastic points distribution in the of the aggregate-subgrade system subjected to higher axle load after strength improvement of the aggregate layer

- **Step 12**: As the secondary failure is still encountered in the subgrade, the final shear strength parameters are not achieved, and the design is progressed to Step 13.
- **Step 13**: In order to tackle the secondary stresses developed in the subgrade, the subgrade cohesion ($c_{subgrade,min}$ = 1.82 kPa) is heuristically and iteratively modified to a higher value $c_{sagg,min}$ = 4 kPa
- **Step 14**: It is observed with $c_{sagg,min}$ = 4 kPa, the unpaved road structure does not fail under vehicular loading. Fig. 16 shows the incremental deviatoric strain diagram after increasing the strength of subgrade layer. It can be observed that the slip lines are prevented from developing prominently in the subgrade layer, and are being primarily confined within the aggregate-subgrade interface.

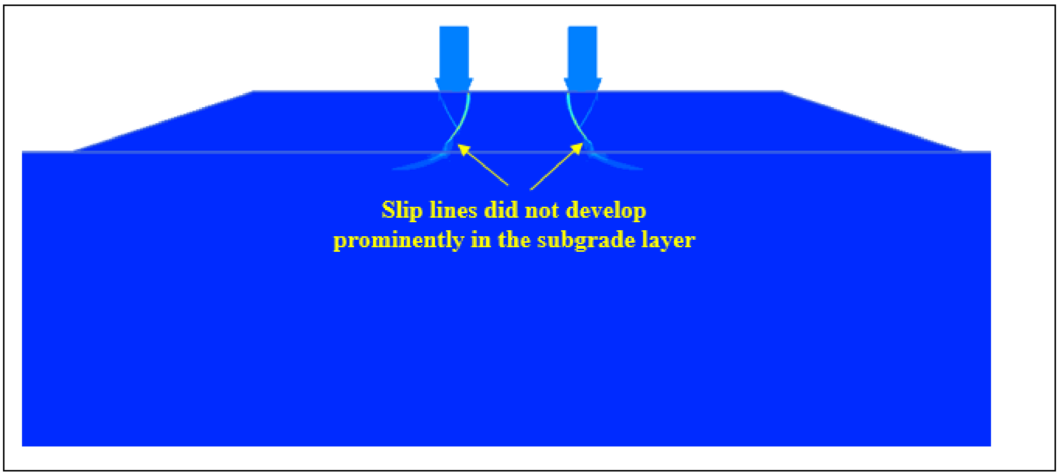

Fig. 16 Response of unpaved road subjected to vehicle loading in terms of incremental deviatoric strain developed in the system while considering the improved strength parameter of subgrade

- **Step 15**: Since the stability against secondary stresses is achieved, the design of unpaved roads is deemed complete with the strength parameters of unpaved road system is finalized to $\varphi_{subgrade}$ = 5° and $c_{sagg,min}$ = 4 kPa as the shear strength parameters for the subgrade, along with $\varphi_{aggregate}$ = 25° and $c_{aggregate,min}$ = 15.56 kPa as the shear strength parameter for the aggregate.

5.1.2 Outcomes from a typical FE-based simulation for Reinforced unpaved road

In Section 5.1.1, a step-by-step design methodology of unpaved roads is discussed. In Step 3, it was observed that under aggregate loading, the subgrade layer undergoes failure. In this regard, strength parameter of the subgrade layer was increased to stabilize the system. In Step 7, under vehicular loading, aggregate layer experienced punching failure. To counteract that, as the strength parameters of the aggregate layer was increased, secondary stresses were transferred to the subgrade layer, thereby necessitating further increase in strength properties of the subgrade. Thus, for an unpaved road structure founded on deformable weak subgrade, additional ground improvement might be required to strengthen the unpaved road system under operational conditions. Depending upon the requirement, different types of traditional ground improvement techniques can be adopted based upon mechanical stabilization that aims to either compact the soils at the surficial regions or until larger depths. The depth of improvement required can be decided from the depth of slip lines formed in the subgrade. Surficial improvement techniques primarily involve compaction by the usage of different types of rollers and heavy weight drops or confides to soil replacement techniques where a portion of the existing subgrade soil can be replaced or blending by soils of better engineering characteristics. Soil improvement to larger depths are generally achieved by the advanced techniques of vibrocompaction, vibroflotation, blast-induced compaction or dynamic compaction accompanied by displacement piles. Soil stabilization using admixtures such as cement, lime, flyash, bitumen and fly-ash are other common adaptations [45, 46]. The selection of ground improvement techniques depends on several factors such as type of soil, geographical structure, seepage conditions, degree of improvement required, availability of equipment and material, available construction time, durability and reusability of materials used, environmental conditions, and finally the cost of project which might be a decisive one. These factors increase the overall cost of construction and consumption of raw materials for the construction. In this regard, inclusion of geosynthetics as reinforcement provides a more practical and cost-effective solutions to such problem. At the same time, the solution using geosynthetics also proves to be sustainable in offering a long-term performance of the improved unpaved road system.

In this regard, finite element-based design methodologies were developed for reinforced unpaved roads under different operational conditions for quasi-static condition (as highlighted in Section 4.3.2). In Step 3 of unreinforced design (Section 5.1.1), it was observed that with the considered properties of the parent material, the subgrade was failing under aggregate loading. As a result, strength parameter of the subgrade layer had to be increased from 1 kPa to 1.82 kPa. However, instead of increasing the strength parameter, a layer of woven geotextile can be placed at the interface of aggregate-subgrade to harness the benefits of introducing a tensile element in the deformable system. The stiffness of the geotextile is considered to be 400 kN/m. It is observed that due to the inclusion of geotextile, model does not undergo failure. Fig. 17a shows the total deviatoric strain diagram after the inclusion of the geosynthetic layer. It can be observed that most of the strains are concentrated at the interface due to the geosynthetic layer and the maximum value is almost half of that unreinforced case. Fig. 17b shows the displacement in the geotextile layer under aggregate loading. It is observed that under aggregate load, the deformed shape of the geotextile is more alike to a trapezoid, and is in contrast to the parabolic form as discussed in earlier studies [20]. The earlier studies have considered the incompressibility of the subgrade soil. It was assumed that the volume of soil displaced downwards due to the settlement below the wheel loading is equal to the volume of soil displaced upwards by heaving between the two wheels. Under this scenario, the geotextile was assumed to attain a wavy parabolic shape upon its deformation. However, earlier studies did not consider any deformation as they followed limit equilibrium approach. The current study considers the coupled stress-deformation approach, wherein the actual deformation of the geotextile is dependent on the stress distribution and corresponding deformation in the subgrade as well. Hence, a different trapezoidal shape of the deformed geotextile is noted in this case. With increase in stiffness, the geotextile can sustain more stresses coming from the aggregate layer and reduces the stresses transferred to the subgrade; this effect is pertinent the tension membrane phenomenon of stretched geotextile.

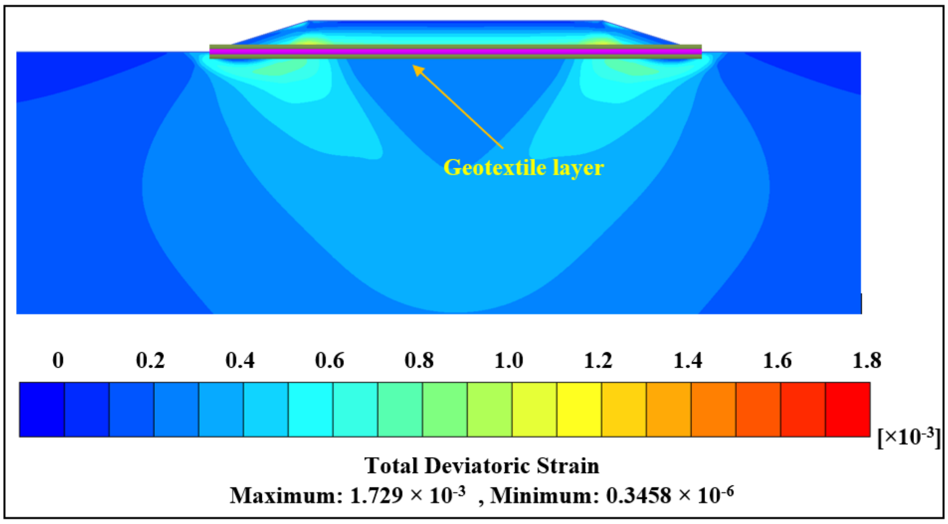

(a)

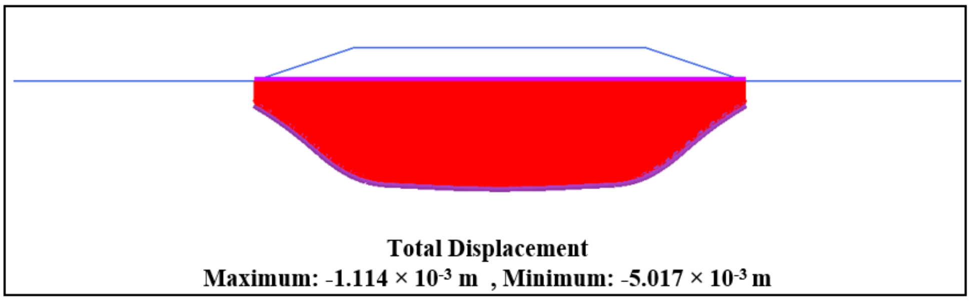

(b)

Fig. 17 Response of the subgrade layer under aggregate loading with a geotextile layer at the interface: (a) Total deviatoric strain (b) vertical displacement in the geotextile layer

In Step 7 for the unreinforced model, due to vehicular loading, punching failure in aggregate layer was observed. As a result, the strength parameter of the aggregate layer was increased to 15.56 kPa from the nominal magnitude. Although the aggregate layer exhibited resistance against the vehicular load, secondary stresses were developed in the subgrade layer of the unpaved road system, thereby destabilizing the unpaved road system. The final strength parameter adopted to strengthen the subgrade layer had to be increased up to 4 kPa. This implies that under vehicular loading, further ground improvement might be required to strengthen the subgrade layer. Hence, as shown in Fig. 18, as an alternative, a geosynthetic layer is included at the aggregate-subgrade interface. The parent material properties are considered as the same discussed in previous section for unreinforced unpaved road under quasi-static condition. The aggregate layer has cohesion value of 15.56 kPa to resist the punching failure stresses in aggregate. The geosynthetic layer is introduced to counter act the secondary stresses developed in the subgrade due to the vehicular loading.

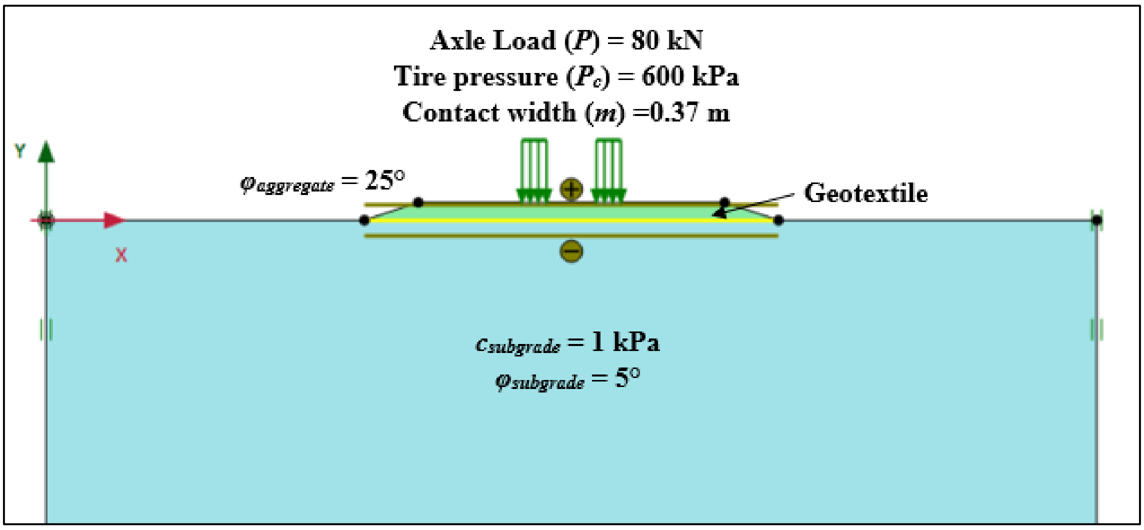

Fig. 18 FE model of geotextile reinforced unpaved road subjected to vehicular load

Initially, the stiffness of the geosynthetic layer is considered to be 400 kN/m and the model is analysed. Fig. 19a shows the incremental deviatoric strains in the analysed model. It is observed that although a layer of geotextile is introduced, the failure lines are still developed in the subgrade, thereby the purpose of reinforcement usage in the unpaved road system is defeated. Hence, the FE model is further analysed with a higher stiffness of geotextile, i.e. 1000 kN/m. Fig. 19b shows with increase in the stiffness of geotextile, maximum strain value reduced by half. However, prominent slip lines within the subgrade layer are still evident and model is observed to exhibit failure. It signifies that for unpaved road built on soft soil and subjected to higher axle loads, the stability is not completely achieved by using a higher stiffness geosynthetic; some additional ground treatment is also required. In the subsequent analysis, the model possessing enhanced cohesive strength parameter of the soil subgrade as 2.5 kPa exhibit stability (Fig. 19c). The cohesion value is lesser than the unreinforced case i.e. 4 kPa, the reduction in cohesion is due to the reinforcement mechanism of geotextile.

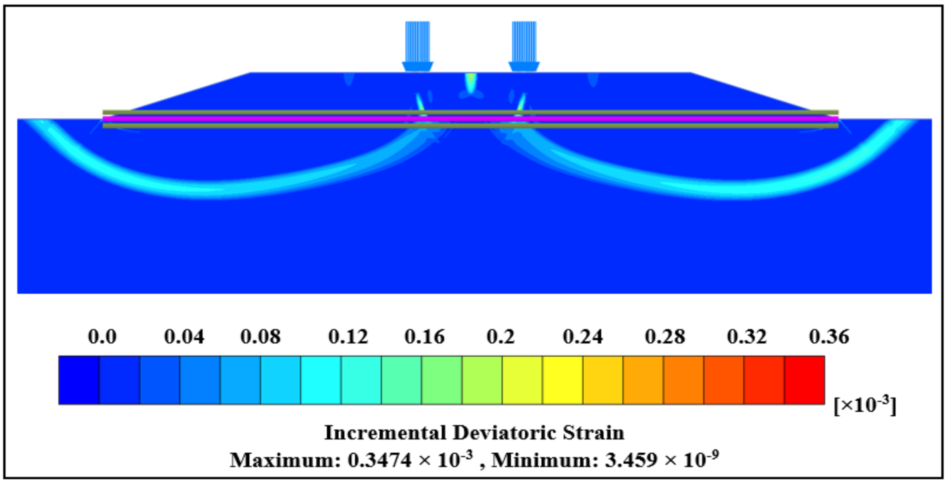

(a)

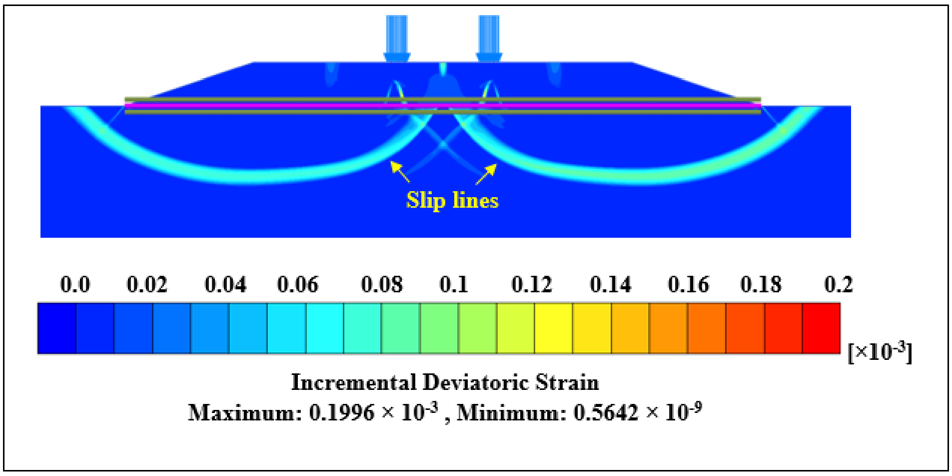

(b)

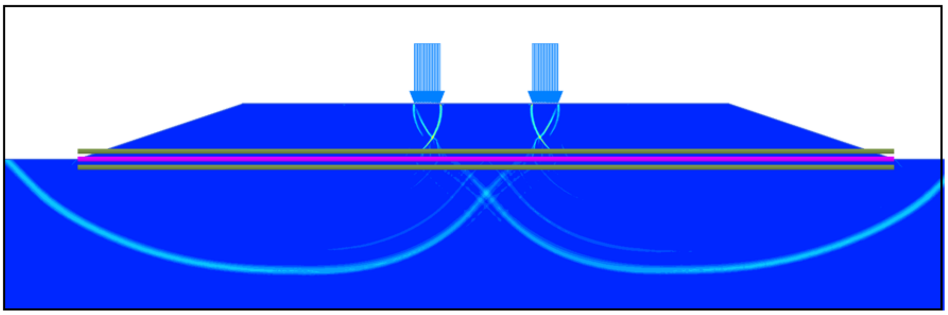
(c)

Fig. 19 Response of the strengthened subgrade layer under vehicular loading with a geotextile layer at the interface and having a stiffness (a) 400 kN/m (b) 1000 kN/m (c) 1000 kN/m

5.1.3 Outcomes from a typical FE-based simulation for reinforced unpaved road with reduced thickness

Unpaved road comprises two layers, the aggregate and the soil subgrade. As understood from previous sections, strength of aggregate layer directly governs the stability of the unpaved road under vehicular loading. The thickness of aggregate layer, estimated from Equation 1, depends on the strength of the subgrade and the magnitude of the applied axle load. For very strong subgrades, the aggregate layer might not be required at all as per the analytical formulation; however, in such case, a nominal aggregate cover of 150 mm is generally provided [20, 21, 47]. For a weaker subgrade or to support a higher axle load or both, a thicker aggregate layer would be required. With thicker aggregate layer, the stability of the unpaved road system is to be supposedly more. This is due to the fact that a thicker aggregate layer is supposed to distribute the wheel stresses over wide area at the aggregate-subgrade interface, thereby leading to reduction in the transferred stress and imparting higher factor of safety against bearing failure. However, depending on the availability of good quality raw aggregates and the associated cost of the same, the cost of construction of an unpaved road also increases for thicker aggregate layers. In this regard, the application of geosynthetic can be a suitable and sustainable option in utilizing a reduced thickness of the aggregate layer, while still attaining the stability of the unpaved road system. The parent material parameters for the analysis are considered as same as that adopted for unreinforced unpaved road condition (Section 5.1.1). Using the adopted parameters, the thickness of the aggregate layer obtained from Equation 1 is 0.79 m. As discussed in the previous section (Section 5.1.1), under operational condition, the aggregate and subgrade undergo failure, as a result the strength parameter of the subgrade and aggregate is modified for a stable unpaved road structure. The final cohesive strength value of subgrade and aggregate are obtained as 15.56 kPa and 4 kPa, respectively. Hence, in a nutshell, the final model parameters for the stable unpaved road section with aggregate thickness of 0.79 m are as follows: P = 80 kN, P_c = 600 kPa, m = 0.37 m, $c_{subgrade}$ = 4 kPa, $\varphi_{subgrade}$ = 5°, $c_{aggregate}$ = 15.56 kPa and $\varphi_{aggregate}$ = 25° and FoS = 1

For the same unreinforced unpaved road model, considering all the enhanced strength of subgrade and aggregate, the thickness of the aggregate layer is intuitively reduced up to 0.6 m and the model is re-analysed. Fig. 20a shows the FE model with reduced aggregate thickness. It is observed that the unpaved road system fails under vehicular load. Fig. 20b shows that the total principal strain diagram shows the migration of strain from aggregate to subgrade, since there is no reinforcing protection at the interface. Fig. 20c shows the development of shear stress concentrations beneath the wheels. Thus, as an overview, due to the reduction in aggregate thickness, the aggregate layer proves to be insufficient in preventing the failure stresses generated by the considered vehicular axle load.

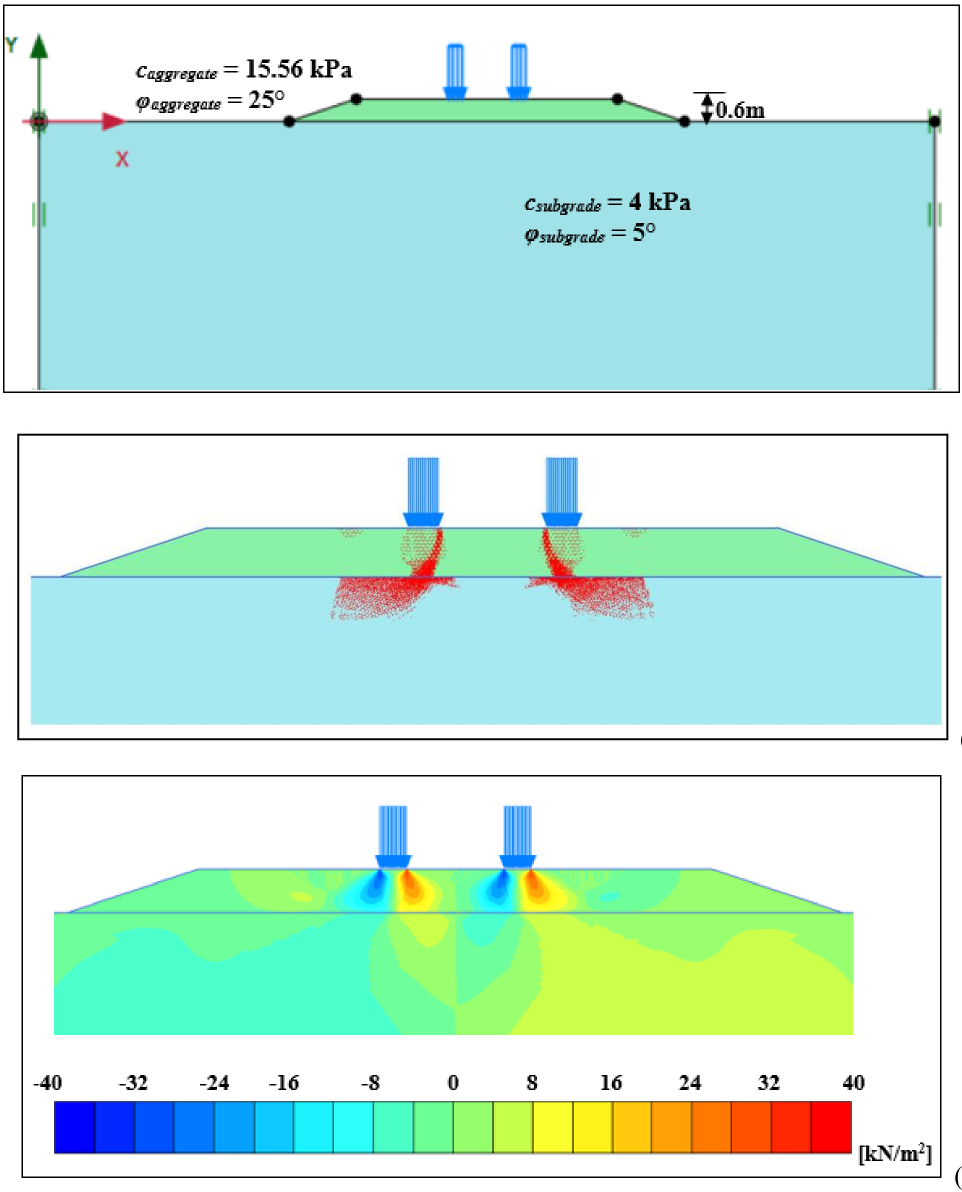

(a)

(b)

(c)

Fig. 20 Response to reduction in thickness of aggregate layer under vehicular loading for unreinforced unpaved road: (a) FE model (b) Total principal strain diagram (c) Development of shear stress concentration in the aggregate layer beneath the wheels

For the same model parameters discussed for the unreinforced case, a geotextile layer is now introduced at the interface of aggregate-subgrade. The axial stiffness of the geotextile layer is chosen as 1000 kN/m. Due to the inclusion of geotextile, the thickness of the aggregate layer can be reduced up to 0.45 m. Beyond 0.45 m, the geosynthetic reinforcing mechanism is not enough to stabilize the unpaved road structure further ground improvement will be required. Fig. 21 shows the incremental deviatoric strain diagram in the reinforced unpaved road section for four different aggregate layer thicknesses i.e. 0.6 m, 0.5 m, 0.45 m and 0.4 m, respectively. Initially, the failure lines are restricted within the aggregate layer; due to the combination of aggregate strength and reinforcing action from the geotextile layer, the slip lines do not develop fully and are conveniently captured at the aggregate-subgrade interface (Fig. 21a). As the thickness is reduced, more stresses are borne by geotextile layer. Until a reduced thickness of 0.45 m (Fig. 21b-c), the slip lines do not develop fully and are well confined within the aggregate layer. However, as the thickness reduced to 0.4 m, distinct slip lines are well developed that passes from the aggregate layer to the subgrade, thereby indicating the failure phenomenon extended within the subgrade even in the presence of geotextile for the cases of aggregate layer with sufficiently reduced thickness (Fig. 21d). Hence, apart from bearing the stresses at the interface, the geotextile layer proves to be sustainable in reducing the thickness of the aggregate layer while achieving the stability of the unpaved road section.

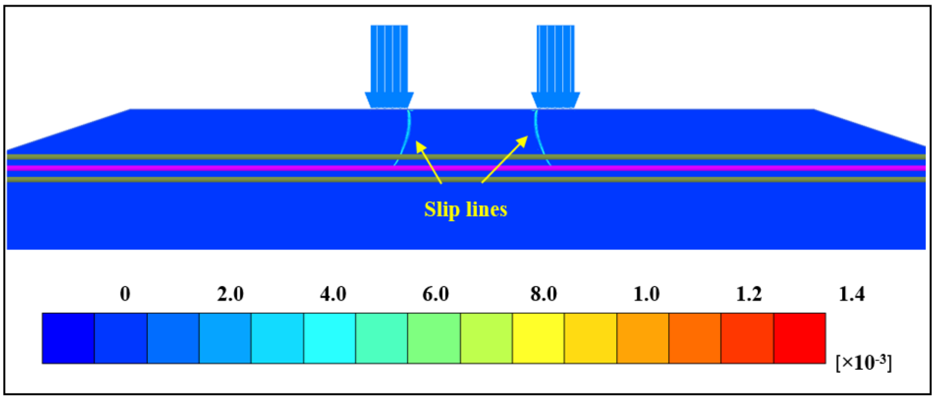

(a)

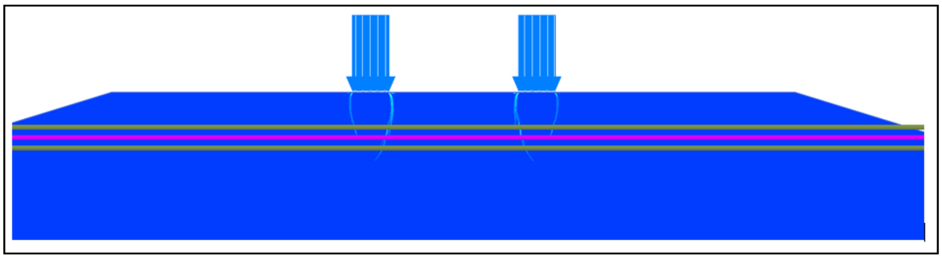
(b)

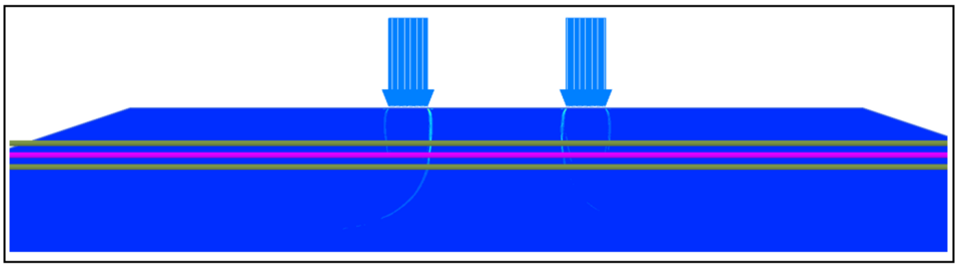
(c)

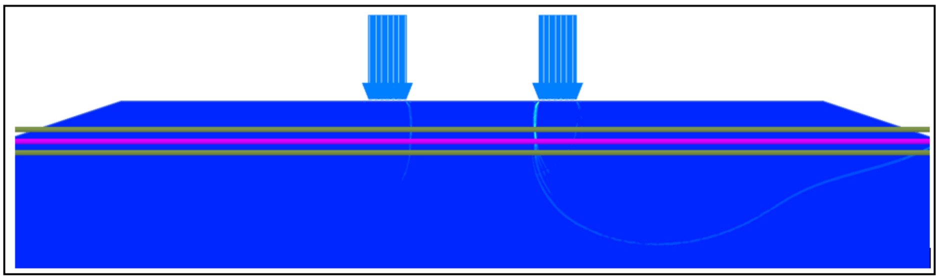

(d)

Fig. 21 Development of incremental deviatoric strains for reinforced unpaved road section as a response to the reduction in thickness of aggregate layer under vehicular loading to: (a) 0.6 m (b) 0.5 m (c) 0.45 m and (d) 0.4 m

5.2 Repetitive Vehicular Loading

In the previous study, sustainable design of geosynthetic reinforced unpaved road based on quasi–static analysis is conducted. Quasi-static analysis represents worst case scenario, considering the vehicle to be almost static and time-independent in nature, thereby imposing the entire weight of the vehicle at a particular location of unpaved road. However, in reality for daily used unpaved roads founded on soft or weak soil subgrade, the overall performance of the road depends on the amount of vehicular load repetition. With gradual increase in the number of loads repetition, permanent damages in the unpaved road structure in the form of rutting is generally observed. A finite element-based design of unpaved road is done to understand how rutting is developed with increase in the number of vehicular load repetition. Later on, the effect of geotextiles of various stiffness are investigated to decipher its sustainability in arresting the rutting developed in the unpaved road section.

The parametric values of the model analysed in this section are as follows: P = 190 kN, P_c = 600 kPa, m =0.56 m, $c_{subgrade}$ = 20 kPa and $\varphi_{aggregate}$ = 35° (Fig. 22). In this model, the subgrade is considered to be comprising weak cohesive soil, while the aggregate is considered to made of purely granular material. Higher axle load is considered so that benefits of using geosynthetics for the critical cases can be understood. Using Equation 1, an unpaved road is modelled with aggregate layered thickness 0.41 m. The model is analysed for three different numbers of vehicle passes: 2 passes, 10 passes and 50 vehicle passes, respectively. In Plaxis 2D, load repetition is described in the form of dynamic load multiplier as illustrated earlier in Section 4.3.2 and in Fig. 8.

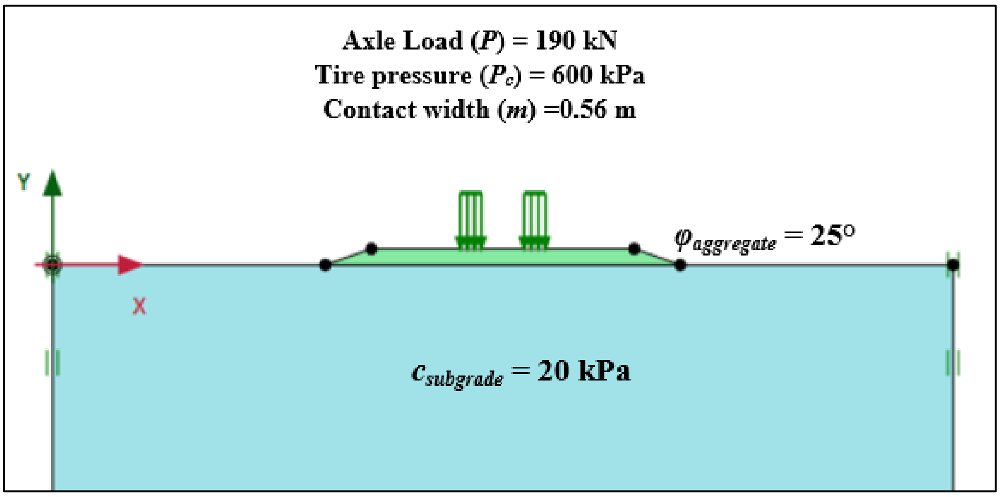

Fig. 22 Typical FE model of unpaved road under repetitive vehicular loading

5.2.1 Outcomes from a typical FE-based simulation for Unreinforced Unpaved Road under Repetitive loading

Fig. 23 shows the amount of rutting developed at the surface of the unpaved road for 2 vehicular passes. The vehicular loading induced rutting in unpaved roads on deformable subgrade is expressed as a combination of maximum settlement beneath the wheels and maximum heaving between the wheels. It is observed from the figure that the maximum heaving is at the central zone, while the settlement is maximum near the edges of the vehicle tire. With increase in the number of vehicular passes, the amount of rut increases significantly. Fig. 24 shows the comparison of rut developed due to 2, 10 and 50 vehicles pass. The rut developed for the mentioned vehicle passes are 0.082 m (comprising heaving of 0.023 m of settlement and 0.059 m of heaving), 0.323 m (comprising heaving of 0.114 m of settlement and 0.209 m of heaving) and 2.02 m (comprising heaving of 0.903 m of settlement and 1.116 m of heaving) respectively. The observations clearly depict that the settlement due to the repeated vehicular load reaches beyond the aggregate layer to the subgrade layer. It is worth mentioning that the rutting reported herein for 50 vehicle passes is a numerical artefact and is not practically reasonable or realistic.

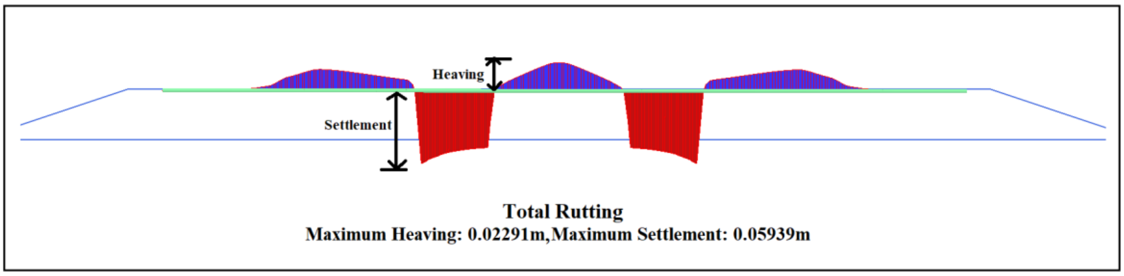

Fig. 23 Rutting developed in unpaved road due to repetitive load from two vehicular cycles

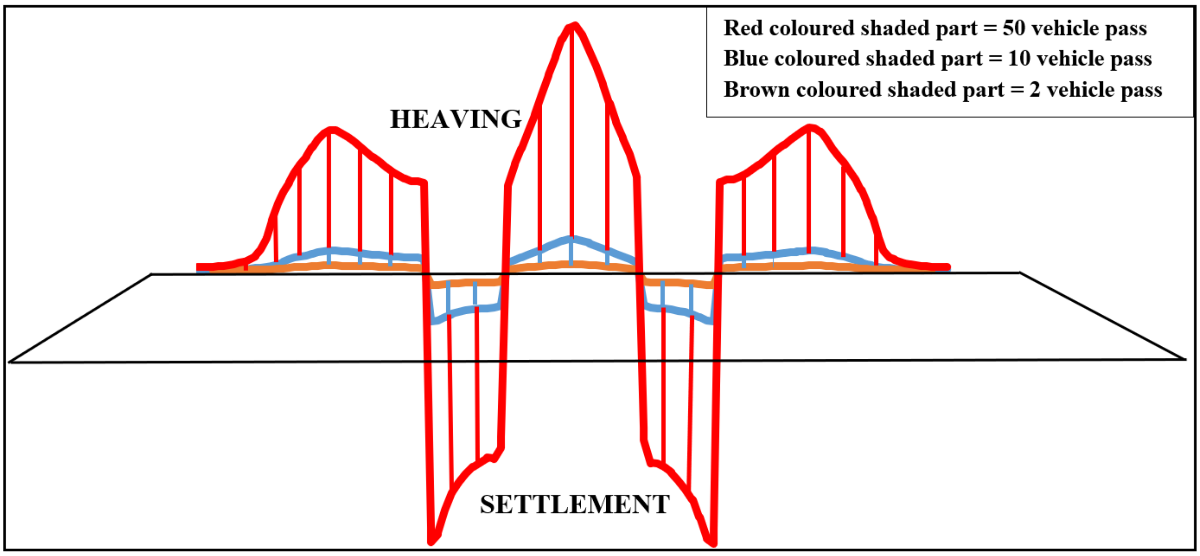

Fig. 24 Comparison of rutting developed in unpaved road due to repetitive load from vehicular cycles comprising 2, 10 and 50 vehicle passes

As mentioned in Section 3, the constitutive behaviour of elastic-perfectly plastic M-C model is capable in addressing the accumulative settlement provided that the yielding occurs at every stage of loading and reloading. For soil elements present in the uppermost levels of the model (having smaller depths from the loading boundary), the confining stresses are small, and hence the yield limits are also on the lower side. As the depth increases, the yield limits would increase with the increase in the confining pressures. Hence, at the lower depths, it is quite customary that each cycle of loading-unloading would lead to gradual accumulation of vertical displacement, with each unloading cycle having some partial elastic recovery. The amount of settlement and accumulation would gradually decrease with depth, and beyond a depth when the yield limit would not be exceeded, the settlements would be purely elastic and no such accumulation would be noticed. This occurs at quite a considerable depth below the surface and is not of importance for the present study. In the present study, all the deformations are measured at the aggregate surface, hence, the accumulation at every loading-unloading-reloading cycles can be observed, which is corroboration to surface rutting phenomenon in roadways. Fig. 25 shows the vertical deformation profile against the dynamic time for 2 vehicular passes at a point directly below the tire wheel. It is observed that the traingular displacement pattern occurs at an interval 0.2 sec, which is similar to the input load multiplier; thereby showing the proper application of input repetitve vehicular load. As the vehicle departs the section, an elastic rebound is noted over a small interval of time until it emerges into a final residual or permanent deformation, i.e. rutting. The elastic rebound occurs for around 0.8 sec after the passage of the vehicular axle load. From the obervations, it can be understood that with each passes, there is an accumualtion of permanent settlement at the surface of unpaved road. After 2 vehicle passes, the permanent vertical deformation is around 50 mm. Similarly, as the number of passes increases, the permanent settlement also increases. For the particular model, after 50 vehicular passes, the total settlement is around 770 mm, which is almost 10 times greater than serviceability criteria of 75 mm.

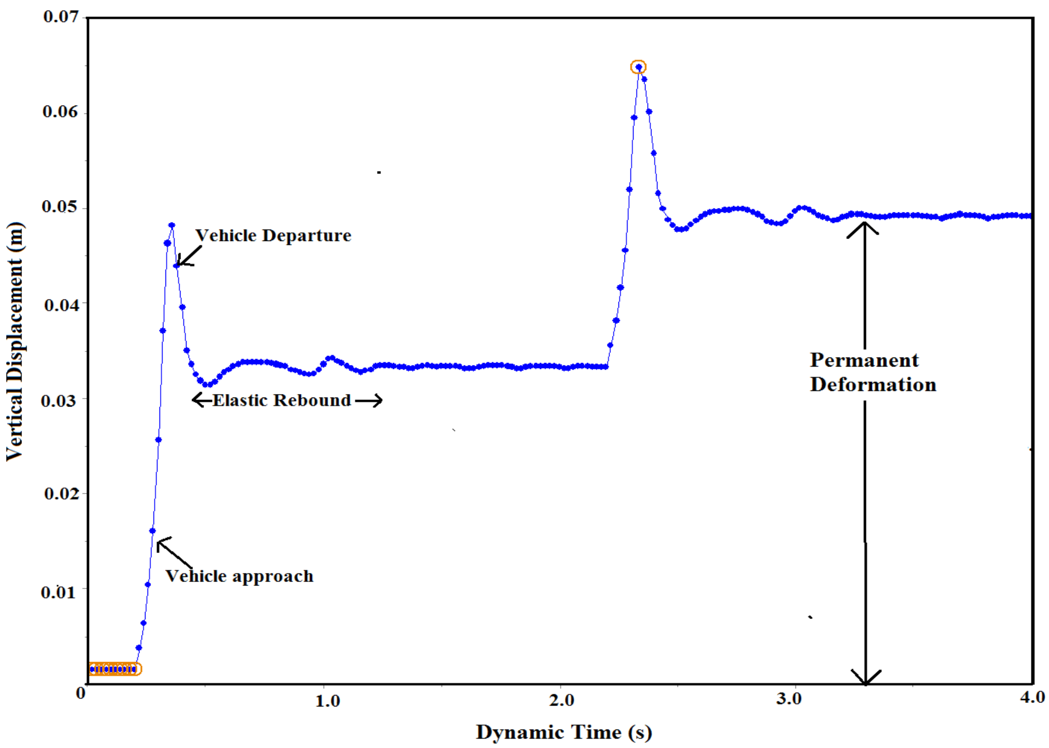

Fig. 25 Vertical deformation profile against dynamic time response of unreinforced unpaved road for 2 cycles of vehicular passes

5.2.2 Outcomes from a typical FE-based simulation for reinforced unpaved road under repetitive vehicular loading

In the previous section, it is understood that for higher axle vehicle load, permanent deformation in the form of rutting develops and it gradually increases with each pass of vehicle and after some passes, the unpaved road system tends to fail on the basis of its serviceability criteria. Rutting not only damages the long-term performance of unpaved road, thereby increasing the regular maintenance cost, it also restricts the day-to-day comfort of commuters depending on the service of the road. In this regard, to seek out a sustainable alternative, a geotextile layer is introduced at the interface of aggregate and subgrade to reduce the rutting developed in unpaved road due to repetitive vehicular loading. The geotextile used in the model is an elastic-isotropic one, whose main material property is defined through its axial stiffness (*EA*). The response of unpaved road under repetitive vehicular load is checked for two different axial stiffness of the geotextile, i.e. 600 kN/m and 1000 kN/m respectively. The parametric properties of the model are kept same as that of the unreinforced case (as illustrated in Section 5.2.1).

Fig. 26 shows the comparison of rutting developed between unreinforced and reinforced unpaved road due to 50 vehicle passes. For a geotextile with axial stiffness 600 kN/m, maximum heaving and maximum settlement are obtained to be 0.377 m and 0.432 m respectively (adding to a rutting of 0.81 m), thereby reducing by 60% in comparison to unreinforced case. Similarly, for a geotextile stiffness of 1000 kN/m, maximum heaving and maximum settlement are 0.248 m and 0.159 m (adding to a rutting of 0.41 m), thereby reducing by approximately 72% and 85%, respectively, in comparison to unreinforced case. Thus, it is understood that with increase in geosynthetic stiffness, the overall rutting of the unpaved road system reduces significantly, thereby increasing the service life of the system. Hence, placement of geotextile reinforcement can be considered a sustainable solution for enhancing the life-period of unpaved roads.

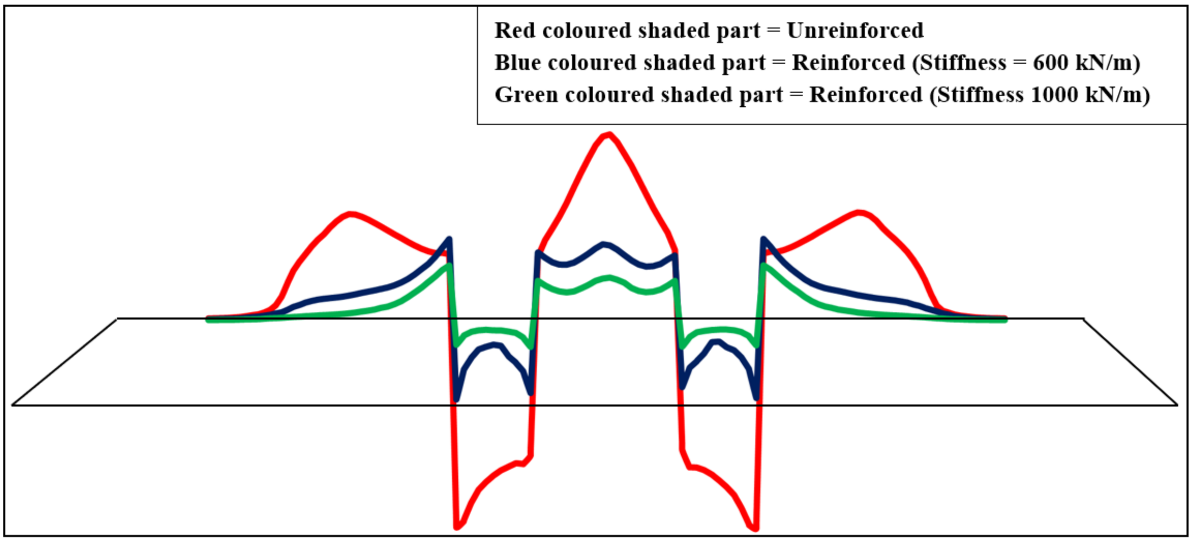

Fig. 26 Comparison of rutting developed between unreinforced and geotextile reinforced unpaved road due to repetitive vehicular load of 50 cycles

Fig. 27 shows the vertical displacement against the dynamic time for the unpaved road system. As discussed earlier, for unreinforced case, for higher axle repetitive load there is a gradual but substantial increase in permanent deformation after each vehicular cycle. It is noted that after 50 vehicular cycles, the permanent deformation is around 770 mm, which is almost 10 times greater than serviceability criteria [20, 21, 41].

Fig. 27 also exhibits the same plot for reinforced unpaved road with geotextile having axial stiffness of 600 kN/m. It is observed that in contrast to the substantial accumulation of rutting for unreinforced case, the vertical deformation-dynamic time curve is largely flatter, thereby indicating the reinforcing action of geosynthetic. The curve shows a gradual increase in permanent deformation with vehicular passages; however, after few cycles, the rutting becomes almost constant. The final permanent deformation after 50 cycles for this case is observed to be approximately 100 mm. For a geotextile having axial stiffness of 1000 kN/m, it is observed that after few initial cycles, the increase in the permanent deformation is restricted totally, and the magnitude of rutting become constant. From the plot, it can be predicted that for reinforced unpaved road with stiffness of geotextile layer being 1000 kN/m, there would not be any change in the permanent deformation beyond 50 vehicular passes. The final permanent deformation after 50 cycles is observed to be approximately 48 mm, which is lesser than the serviceability criteria of 75 mm.

Fig. 27 comprehensibly delineates the beneficial and sustainable application of geotextile in arresting the vertical deformation in unpaved road system. Geotextiles, with properly chosen axial stiffness, not only substantially reduces the rutting in comparison to the unreinforced unpaved roads, it would be also largely successful in arresting the rutting and preventing the accumulation of rutting under larger number of vehicular load cycles. This transcribes to that understanding that properly chosen geotextile and their proper implementation in the construction practices of unpaved roads can significantly enhance the performance and sustainability of the same.

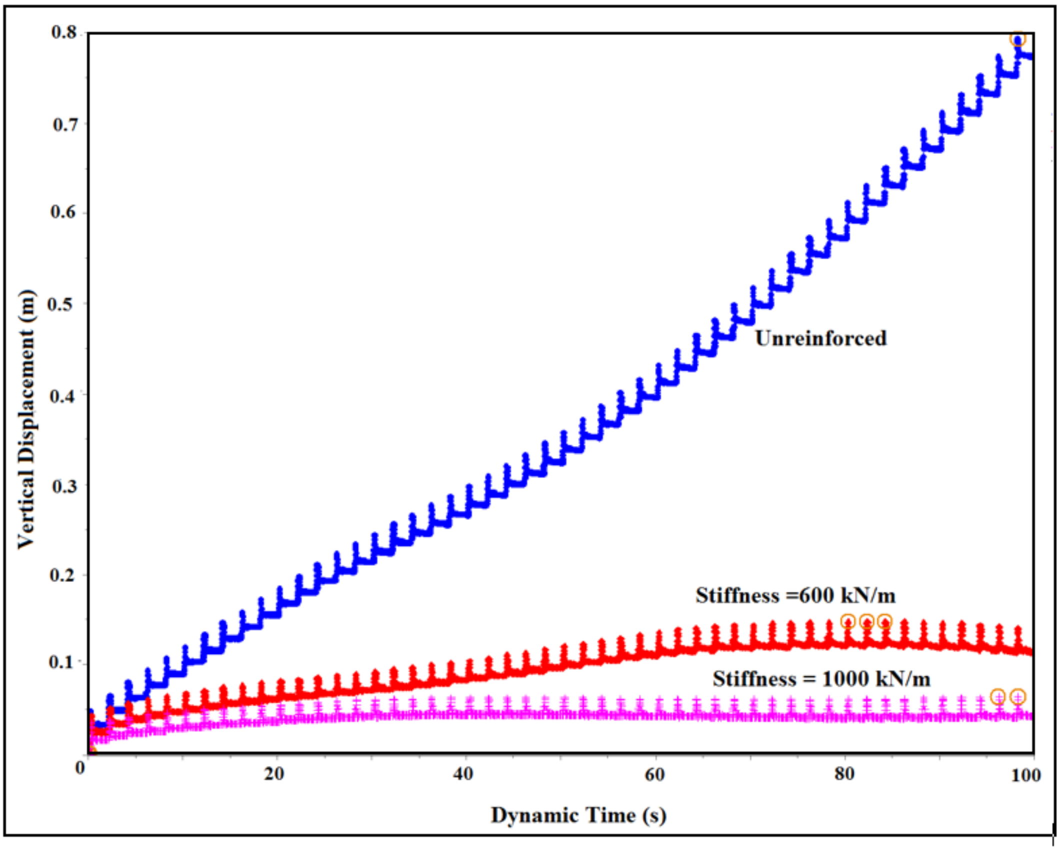

Fig. 27 Comparison of rutting of unreinforced and geotextile reinforced unpaved road for 50 vehicular passes using geotextiles of varying axial stiffness

6.0 Conclusions and Recommendations

This paper illustrates the necessity of using geotextile as reinforcement in design of unpaved road resting on weak deformable soft soil with the aid of a coupled stress-deformation based approach. Conventional limit equilibrium based approach considered the individual component of unpaved road are non-deformable, that eventually leads a conservative design. Therefore, a FE based stress-deformation approach is considered in this study to simulate the real field behaviour of unpaved roads under vehicular axle load. The paper produced the results for both unreinforced and geotextile reinforced unpaved road under quasi-static and repetitive loading conditions. The benefits of using geosynthetic in overall stability of the unpaved road under different operational conditions is administered. Following are the list of important outcomes from the present study:

- A FE-based step-by-step design methodology of unpaved road resting on generalized weak soil subgrade under quasi-static loading condition is produced. The coupled stress-deformation based design gives the response of unpaved road section for different operational conditions i.e., failure of subgrade under aggregate loading and failure of aggregate under quasi-static vehicular loading. Such operational conditions are not considered in the conventional design of unpaved roads. Through the FE-based design, the necessity of improvement in strength of the individual component of the unpaved road is illustrated so that the operational failures can be suitably averted.
- Introduction and application of geotextiles at the aggregate-subgrade interface leads to substantial improvement of the unpaved road system over its unreinforced state. For unpaved roads resting on weak soil subgrade, inclusion of geotextile having even lower axial stiffness is enough to counteract the stresses coming from aggregate loading and prevent the corresponding operational failure. Utilization of geotextile proves to be a suitable and sustainable alternative in comparison to the conventional and commonly adopted in-situ ground modification techniques to improve the subgrade of unreinforced unpaved roads.
- Application of geotextile is also found to be largely beneficial in arresting the secondary stresses at the aggregate-subgrade interface that are originated due to simultaneous loading from aggregate layer and vehicular passes.
- Application of geotextile reinforcement at aggregate-subgrade interface proves effective in reducing the thickness of the aggregate cover in comparison to that required in the unpaved roads. For unreinforced case, a reduction in aggregate thickness leads to the migration of the strains from the aggregate to the subgrade layer, thereby leading to rutting induced failure. However, utilization of geotextile at the interface effectively arrests the stresses generated by the vehicular load, as a result of which a reduction in the aggregate thickness can be comfortably achieved up to 45%-50% of the thickness required for an unreinforced unpaved road.
- FE model developed for unpaved road built on weak soil subgrade is analysed under repetitive vehicular loading. The output results depict that the rutting behaviour of the unpaved road under multiple vehicle passes is well represented. With increase in number of vehicle passes, the rutting in the unpaved road increases. For specific cases of model parameters, the plot between vertical displacement and dynamic time revealed that after larger number of load repetitions (≥ 50), the total permanent settlement

accumulated at the surface of unpaved road might significantly exceed the serviceability criteria, thereby rendering the unpaved road unusable in long run.

- The surface rutting in an unpaved road is significantly reduced by incorporating a geotextile layer at the interface of the aggregate and subgrade, which depends on the axial stiffness of the chosen geotextile. For a typical unpaved road system, a geotextile with higher axial stiffness, such as 1000 kN/m, is capable of reducing the rutting by almost 85% to that obtained for an unreinforced scenario.
- Geotextile with higher axial stiffness not only limits the rutting below the serviceability criteria, it is also capable of restricting the rutting from further accumulation even with higher number of vehicular passes. For a typical unpaved road system, a geotextile with axial stiffness of 1000 kN/m exhibited a restriction on the accumulation of rutting induced deformation even higher numbers of vehicular passes. The rutting is found to attain constant magnitude beyond 40 cycles, and the same is maintained for even 100 cycles. This indicates that the application of geotextile with a properly chosen axial stiffness is sustainable enough to completely prevent progressive rutting for significantly higher number of vehicle passes over the unpaved road system.

With increase in global population and industrialization the demand of global transportation network is tremendously increasing. This rapid growth in urbanization, supplemented by depletion of global natural reserve of good quality raw material and communication routes with sufficient bearing capacity, many a times leads to the construction of unpaved roads over weak and highly deformable subsoil conditions. With the growth in vehicle numbers, the number of passes of vehicle over a particular section of road has also significantly increased. Added to that, the use of poor quality of locally available marginal materials as aggregates also hampers the long-term performance of unpaved roads that starts exhibiting significant and uncontrollable rutting. Conventionally adopted ground improvement proves to be costly when it is adopted for long stretches of road network. In this regard, use of geosynthetic proves to be sustainable solution offering durability and long-term performance of the unpaved road by controlling the rutting within serviceability criteria and not allowing the rutting to progressively accumulate with increasing number of vehicles passes.

7.0 Future Scope of the Present Research

This paper successfully highlights the fruitful application of a single layer of geotextile at the aggregate-subgrade interface and illustrates that a properly chosen axial stiffness of the geotextile is largely sufficient in imparting sustainability to a technical safe design of unpaved roads. In this regard, depending on the strength characteristics of natural soil subgrade and the aggregate material, application of multiple layers of geotextiles within the subgrade and aggregate can also be explored to explore and harness their benefit in enhancing the sustainability and longevity of the unpaved roads. Further, the design approach prescribed herein utilizes a single quasit-static vehicle load at the center of the roadway section. Presence of mixed traffic scenario and moving along the different sections of the road should be thoroughly analysed to understand the response of the designed section.

Funding Statement

This research did not receive any specific grant from funding agencies like public, commercial or non-profit sectors.

Conflict of Interest

The authors declare that they have no conflict of interest.

References

1. Faiz AJ (2012) The promise of rural roads: Review of the role of low-volume roads in rural connectivity, poverty reduction, crisis management, and livability. In Transportation Research Circular; Transportation Research Board, Washington, DC, USA.
2. MORTH (2023) Ministry of Road Transport and Highways. Government of India. https://morth.nic.in/sites/default/files/RTYB-2017-18-2018-19. Accessed 6th June 2023.
3. CIA (2023) The world fact book, field listings – Roadways. https://www.cia.gov/the-world-factbook/countries/united-states. Accessed 6th June 2023.
4. FHWA (2015) Gravel roads construction and maintenance guide. Federal Highway Authority of America, U.S. Department of Transportation, Washington DC, USA.
5. Paige-Green P, Pinard M, Netterberg F (2015) A review of specifications for lateritic materials for low volume roads. Transp Geotech 5:86-98. http://dx.doi.org/10.1016/j.trgeo.2015.10.002
6. Mendoza A, Guaje J, Enciso C, Beltran G (2022) Mechanical behavior assessment of tire-reinforced recycled aggregates for low traffic road construction. Transp Geotech 33:1-8. https://doi.org/10.1016/j.trgeo.2022.100730
7. Leonardi G, Bosco DL, Palamara R, Suarci F (2020) Finite element analysis of geogrid-stabilized unpaved roads. Sustainability 12(5):1-11. https://doi.org/10.3390/su12051929
8. Richards RG (1978) Lightly trafficked roads in southern Africa. A review of practice and recommendations for design. Pretoria, South Africa.
9. Shoop S, Haehnel R, Janoo V, Harjes D, Liston R (2006) Seasonal deterioration of unsurfaced roads. J Geotech Geoenviron Eng ASCE 132(7):852-860. https://doi.org/10.1061/(ASCE)1090-0241(2006)132:7(852)
10. Jones D, Paige-Green P (2015) Limitations of using conventional unpaved road specifications for understanding unpaved road performance. Transp Res Rec 2474(1):30-38. https://doi.org/10.3141/2474-04
11. Le Vern M, Razamkamantsoa A, Murzyn F, Larrarte F, Cerezo V (2022) Effects of soil surface degradation and vehicle momentum on dust emissions and visibility reduction from unpaved roads. Transp Geotech 37:1-12. https://doi.org/10.1016/j.trgeo.2022.100842
12. Ibagon L, Caicedo B, Villaceres JP, Yepez F (2023) Modelling of washboard effect on unpaved roads experimental evidence on non-cohesive materials. Transp Geotech 41:101015. https://doi.org/10.1016/j.trgeo.2023.101015
13. Fannin RJ, Sigurdsson O (1996) Field observations on stabilization of unpaved roads with geosynthetics. J Geotech Eng ASCE 122(7):544-553. https://ascelibrary.org/doi/10.1061/%28ASCE%290733-9410%281996%29122%3A7%28544%29
14. Calvarano LS, Palamara R, Leonardi G, Moraci N (2016) Unpaved Road reinforced with geosynthetics. Proce Eng 158:296-301. https://doi.org/10.1016/j.proeng.2016.08.445

15. Buonsanti M, Leonardi G, Scopelliti F (2012) Theoretical and computational analysis of airport flexible pavements reinforced with geogrids. In: Proceeding 7th RILEM International Conference on Cracking in Pavements, Volume 4, pp 1219–1227.
16. Calvarano LS, Leonardi G, Palamar R (2017) Finite element modelling of unpaved road reinforced with geosynthetics. Proce Eng 189:99 –104. https://doi.org/10.1016/j.proeng.2017.05.017
17. Bayraktar OY (2020) Use of geosynthetics in road construction. J Eng Sc 6(2):107-113.
18. Vaitkus A, Siukscius A, Ramūnas V (2014) Regulations for use of geosynthetics for road embankments and subgrades. Baltic J Road Bridge Eng 9(2):88–93. https://bjrbe-journals.rtu.lv/article/view/bjrbe.2014.11
19. Singh M, Trivedi A, Shukla SK (2022) Evaluation of geosynthetic reinforcement in unpaved road using moving wheel load test. Geotex Geomem 50(4):581–589. https://doi.org/10.1016/j.geotexmem.2022.02.005
20. Giroud J, Noiray L (1981) Geotextile-reinforced unpaved road design. J Geotech Eng Div ASCE 107(9):1233-1254. https://ascelibrary.org/doi/10.1061/AJGEB6.0001187
21. Holtz R, Sivakugan N (1987) Design charts for roads with geotextiles. Geotext Geomembranes 5(3):191-199. https://www.sciencedirect.com/science/article/abs/pii/0266114487900161
22. Bourdeau PL, Holtz RD, Chapuis J (1988) Effect of anchorage and modulus in geotextile-reinforced unpaved roads. Geotex Geomem 7(3):221-30. https://doi.org/10.1016/0266-1144(88)90010-6
23. Douglas RA, Kelly MA (1986) Geotextile reinforced unpaved logging roads: The effect of anchorage. Geotex Geomem 4(2):93-106. https://doi.org/10.1016/0266-1144(86)90018-X
24. Milligan G, Jewell R, Houlsby G, Burd H (1989a) A new approach to the design of unpaved roads – Part I. Ground Eng 22(3):25-29. https://cdn.ca.emap.com/wp-content/uploads/sites/13/1989/11/1989-11_Pages_37-42.pdf
25. Milligan G, Jewell R, Houlsby G, Burd H (1989b) A new approach to the design of unpaved roads – Part II. Ground Eng 23(8):37-42. https://cdn.ca.emap.com/wp-content/uploads/sites/13/1989/11/1989-11_Pages_37-42.pdf
26. Tingle JS, Webster SL (2003) Corps of engineers' design of geosynthetic-reinforced unpaved roads. Transp Res Rec 1849(1):3-230. https://doi.org/10.3141/1849-21
27. US Army Corps of Engineers (1995) Engineering use of geotextiles. Army Technical Manual TM 5-818-8 (Air Force Joint Manual AFJMAN 32-1030). Headquarters, U.S. Departments of the Army and Air Force.
28. Giroud JP, Han J (2004a) Design methods for geogrid-reinforced unpaved roads I-Development of design method. J Geotech Geoenviron Eng ASCE 130(8):775-786. https://doi.org/10.1061/(ASCE)1090-0241(2004)130:8(775)
29. Giroud JP, Han J (2004b) Design methods for geogrid-reinforced unpaved roads II-Calibration and application. J Geotech Geoenviron Eng ASCE 130(8):787-797. https://doi.org/10.1061/(ASCE)1090-0241(2004)130:8(787)
30. Hufenus R, Rueegger R, Banjac R, Mayor P, Springman SM, Bronnimann R (2006) Full-scale field tests on geosynthetic reinforced unpaved roads on soft subgrade. Geotext Geomembranes 24(1):21–37. https://doi:10.1016/j.geotexmem.2005.06.002

31. Lyons CK, Fannin J (2006) A comparison of two design methods for unpaved roads reinforced with geogrids. Can Geotech J 43:1389-1394. https://cdnsciencepub.com/doi/10.1139/t06-075
32. Perkins SW, Christopher BR, Lacina BA, Klompmaker J (2012) Mechanistic-empirical modeling of geosynthetic-reinforced unpaved roads. Int J Geomech ASCE 12(4):370-380. http://dx.doi.org/10.1061/(ASCE)GM.1943-5622.0000184
33. Han B, Ling J, Shu X, Song W, Boudreau RL, Hu W, Huang B (2019) Quantifying the effects of geogrid reinforcement in unbound granular base. Geotex Geomem 47(3):369–376. https://doi.org/10.1016/j.geotexmem.2019.01.009
34. Meena S, Choudhary L, Dey A (2013) Quasi-static analysis of geotextile-reinforced unpaved road resting on *c-φ* subgrade. Proce- Soc Behav Sci 104:235–244. https://doi.org/10.1016/j.sbspro.2013.11.116
35. Vern ML, Doré G, Bilodeau JP (2016) Mechanistic-empirical design of unpaved roads. In: TAC 2016-Efficient Transportation-Managing the Demand, 2016 Conference of the Transportation Association, Toronto, Canada.
36. Zarnani S, Bathurst RJ (2008) Numerical modeling of EPS seismic buffer shaking table tests. Geotex Geomem 26:371-383. https://doi.org/10.1016/j.geotexmem.2008.02.004
37. Labuz JF, Zhang A (2012) Mohr-Coulomb failure criterion. Rock Mech Rock Eng 45:975-979. https://doi.org/10.1007/s00603-012-0281-7
38. Cui XZ, Jin Q, Shang QS, Liu ST (2006) Mohr-Coulomb model considering variation of elastic modulus and its application. Key Eng Mat 306-388:1445-1448. https://doi.org/10.4028/www.scientific.net/KEM.306-308.1445
39. Zarnani S, Bathurst RJ (2009) Influence of constitutive model on numerical simulation of EPS seismic buffer shaking table tests. Geotex Geomem 27:308-312. https://doi.org/10.1016/j.geotexmem.2008.11.008
40. Zarnani S, El-Emam MM, Bathurst RJ (2011) Comparison of numerical and analytical solutions for reinforced soil wall shaking table tests. Geomech Eng 3(4):291-321. https://doi.org/10.12989/gae.2011.3.4.291
41. Lade PV (2005) Overview of constitutive models for soils. In: Geotechnical Special Publications No. 128, pp 1-34.
42. Yaghoubi E, Arulrajah A, Wong Y, Horpibulsuk S (2016) Stiffness properties of recycled concrete aggregate with polyethylene plastic granules in unbound pavement applications. J Mat Civil Eng ASCE 29(4):04016271-1-7. https://doi.org/10.1061/(ASCE)MT.1943-5533.0001821
43. Ghosh P, Kumar S (2011) Interference effect of two nearby strip surface footings on cohesionless layered soil. Int J Geotech Eng 5(1):87-94. https://doi.org/10.3328/IJGE.2011.05.01.87-94
44. Terzaghi K (1943) Theoretical Soil Mechanics. John Wiley and Sons, New York, USA.
45. Kirsch K, Bell A (2013) Ground Improvement. CRC Press, Boca Raton, USA.
46. Chattopadhyay BC, Maity J (2017) Ground Improvement Techniques. PHI, New Delhi, India.
47. IRC: SP-72 (2015) Guidelines for the design of flexible pavements for low volume rural roads. Indian Road Congress, New Delhi